ORCA – Online Research @ Cardiff

1   **Dual role of Mucosal-Associated Invariant T cells in type 1 diabetes**

2

3   Ophélie Rouxel[1,2,3*], Jennifer DaSilva[1,2,3*], Lucie Beaudoin[1,2,3*], Isabelle Nel[1,2,3], Céline

4   Tard[1,2,3], Lucie Cagninacci[1,2,3], Badr Kiaf[1,2,3], Masaya Oshima[1,2], Marc Diedisheim[1,2], Marion

5   Salou[11], Alexandra Corbett[7], Jamie Rossjohn[4,5,6], James McCluskey[7], Raphael Scharfmann[1,2],

6   Manuela Battaglia[8], Michel Polak[1-2;9-10], Olivier Lantz[11], Jacques Beltrand[9-10], Agnès

7   Lehuen[1,2,3].

8   **Author Affiliations:** [1]INSERM U1016, Institut Cochin, Paris, France and Université Paris

9   Descartes; [2]CNRS, UMR8104, Paris, France. [3]Laboratoire d'Excellence INFLAMEX, Sorbonne

10   Paris Cité, France; [4]ARC Centre of Excellence in Advanced Molecular Imaging, [5]Infection and

11   Immunity Program and Department of Biochemistry and Molecular Biology, Biomedicine

12   Discovery Institute, Monash University, Clayton, Victoria 3800, Australia; [6]Institute of

13   Infection and Immunity, Cardiff University, Cardiff, UK; [7]Department of Microbiology and

14   Immunology, Peter Doherty Institute for Infection and Immunity, University of Melbourne,

15   Parkville, Australia. [8]Diabetes Research Institute (DRI), IRCCS San Raffaele Scientific Institute,

16   Milan, Italy; TrialNet Clinical Center, San Raffaele Hospital Milan, Italy. [10]Service

17   Endocrinologie, Gynécologie et Diabétologie Pédiatrique, Hôpital Universitaire Necker

18   Enfants Malades, Assistance Publique-Hôpitaux de Paris, Paris, France. [10]Faculté de

19   Médecine Paris Descartes, Université Sorbonne Paris Cité, Paris, France. [11]INSERM U932,

20   Institut Curie, Paris, France.

21

22   **Author Notes:** [*]O. Rouxel, J. DaSilva and L. Beaudoin contributed equally to this paper.

23

24   **Corresponding Author:** Agnès Lehuen, INSERM 1016, Institut Cochin, Paris, France. Phone:

25   +331 76 53 55 90; Fax : +331 46 34 64 54; E-mail : agnes.lehuen@inserm.fr.

Abstract

Type 1 diabetes is an autoimmune disease resulting from the destruction of pancreatic-β cells by the immune system involving innate and adaptive immune cells. Mucosal-associated invariant T (MAIT) cells are innate-like T-cells recognizing bacterial riboflavin-precursor derivatives presented by the MHC-I related molecule, MR1. Since T1D is associated with gut microbiota modification, we investigated MAIT cells in this pathology. In T1D patients and non-obese (NOD) diabetic mice, we detected MAIT cell alterations, including increased granzyme B production, which occur before disease onset. Analysis of NOD mice deficient for MR1, and therefore lacking MAIT cells, revealed a loss of gut integrity, increased anti-islet responses associated with exacerbated diabetes. Altogether our data highlight the role of MAIT cells in the maintenance of gut integrity and the control of anti-islet autoimmune responses. MAIT cell monitoring could represent a new biomarker in T1D while their manipulation may open new therapeutic strategies.

Introduction

Type 1 Diabetes (T1D) is an auto-immune disease characterized by the selective destruction of pancreatic islet β cells producing insulin, in the context of an underlying multigenetic inheritance[1]. When most of the β cells are destroyed or non-functional, the consecutive lack of insulin results in hyperglycemia and requires a life-long insulin replacement therapy[1]. The physiopathology of T1D involves both innate and adaptive immune systems that are inappropriately activated inducing a loss of self-tolerance and islet destruction[2–5]. T1D is characterized by the presence of anti-islet autoantibodies and autoreactive T cells. Innate immune cells are involved at various stages of the disease and are particularly important for the initiation of the local immune response in the pancreas and the pancreatic lymph nodes[2,4]. Recent data have highlighted the role of the intestinal microbiota in T1D by transfer experiments in NOD mice[6–9] and gut microbiota differences in children associated with T1D development[10–12]. Several studies also described gut mucosa alterations in NOD mice and T1D patients[13–17].

MAIT cells are innate-like T cells recognizing bacterial metabolites, derived from the synthesis of riboflavin, presented by the monomorphic major-histocompatibility-complex-

2

class-I-related protein MR1[18–20]. These non-conventional T cells express a conserved αβ-TCR, consisting of an invariant TCRα chain, Vα7.2-Jα33/20/12 in humans and Vα19-Jα33 in mice, with a restricted set of TCRβ chains. MAIT cells produce various cytokines such as TNF-α, IFN-γ, IL-17 and granzyme B (GzB) that could participate to tissue inflammation and cell death[18,21–31]. The near absence of MAIT cells in germ-free mice[18,32] and their physiological localization at mucosal sites including the gut[18,23] suggest a strong interaction with the microbiota. Here for the first time we described MAIT cell alteration in T1D patients and our mouse data reveal the protective role of MAIT cells against T1D. The localization and the function of MAIT cells highlight their key role in the maintenance of gut integrity, thereby controlling the development of autoimmune responses against pancreatic β cells.

Results

Alteration of blood MAIT cell frequency and phenotype in children with recent onset T1D

We first began the investigation of MAIT cells in T1D by analyzing MAIT cell frequency and phenotype in fresh peripheral blood samples from children with recent onset T1D and children with established T1D as compared to age-matched control children (**Supplementary Tables 1 and 2**). MAIT cells can be identified in human blood as CD4⁻ T lymphocyte expressing Vα7.2 TCRα gene segment and CD161^{high19,20,24,33,34} **(Fig. 1a)**. MAIT cell frequency and number was decreased (3-fold) in the blood of recent onset T1D children whereas no significant difference was observed in children with established disease as compared to control children **(Fig. 1a and Supplementary Fig. 1a)**. Decreased frequency was observed in both CD8⁺ and double negative (DN) MAIT cell subsets **(Supplementary Fig. 1b)**. Of note there was no difference in the frequencies of conventional CD4 and CD8 T cells, and of Vα7.2⁺CD161⁻ T cells between the three children populations confirming that the decrease of MAIT cell frequency at the onset of T1D was not secondary to changes in other T cell populations nor to down-regulation of the CD161 marker **(Supplementary Fig. 2a-b)**. Analysis of MAIT cell phenotype showed a decreased frequency of MAIT cells expressing tissue recruitment/adhesion molecules (CCR6, CD56) at the onset of the disease, an increased frequency of MAIT cells expressing the activation/exhaustion markers CD25 and PD1, and a decreased frequency of MAIT cells expressing the anti-apoptotic molecule Bcl-2 **(Fig. 1b-c)**. Multi-parametric analysis of MAIT cells in the children with established T1D

3

89   highlighted the intermediate phenotype of MAIT cells between those from recent onset T1D

90   and control children **(Fig. 1c)**. Interestingly in recent onset children the frequency of MAIT

91   cells expressing migratory CCR6$^+$ or anti-apoptotic Bcl-2 molecules were positively correlated

92   with the frequency of MAIT cells, whereas MAIT cell CD25 expression was negatively

93   correlated with MAIT cell frequency **(Supplementary Fig.3).** These data suggest that

94   decreased blood MAIT cell frequency could reflect their migration to inflamed tissues and/or

95   their death by apoptosis subsequent to their activation.

96

97   **Alteration of blood MAIT cell function in children with recent onset T1D**

98   Cytokine and GzB production by fresh blood MAIT cells was analyzed after PMA-ionomycin

99   stimulation. MAIT cells from children with recent onset T1D produced less IFN-γ, whereas

100   their production of TNF-α, IL-4, and GzB was increased as compared with MAIT cells from

101   control children **(Fig. 2a-b)**. Of note, among these effector molecules only the frequency of

102   GzB correlated with the frequency of MAIT cells, the higher GzB production was observed in

103   patients with the lower frequency of MAIT cells (**Supplementary Fig.4**). Multi-parametric

104   analysis of cytokines and GzB production by MAIT cells also showed an intermediate status

105   of blood MAIT cells from children with established T1D, between those from control children

106   and recent onset T1D children, as already observed for MAIT cell surface phenotype **(Fig.**

107   **2b)**. We next analyzed the ability of MAIT cells to respond to specific TCR activation by the

108   ligand 5-OP-RU[20]. Upon stimulation, MAIT cells from control children up-regulated CD69 and

109   CD25 activation markers. Addition of blocking MR1 mAb confirms that this activation was

110   TCR-dependent. Interestingly, MAIT cell activation was significantly reduced in children with

111   recent onset T1D **(Fig. 2c)**. Together, these results highlight functional alteration of MAIT

112   cells in children with recent onset T1D.

113

114   **Cytotoxic function of MAIT cells on human β cells**

115   We next investigated potential links between phenotype and functional alterations of MAIT

116   cells and clinical characteristics of children with recent onset T1D **(Supplementary Tables 1**

117   **and 2).** Interestingly, the frequency of GzB$^+$ MAIT cells was negatively associated (r=-0.71,

118   P<0.0001) with children's age at diagnosis **(Fig. 3a),** which is in agreement with the current

119   view that T1D is more aggressive in the youngest children[35,36]. We speculate that production

120   of GzB by MAIT cells, reflecting their cytotoxic potential, could be involved in the

physiopathology of T1D. Other MAIT cell parameters, such as their frequency, CCR6 and Bcl-2 expression, were also associated with the age at diagnosis **(Supplementary Fig. 5)**. No significant correlations between MAIT cell parameters and age were observed in controls and children with established T1D (data not shown). Production of GzB by MAIT cells inversely correlated with HbA1c level at the onset of the disease but not in children with established T1D (**Fig. 3a**). Indeed, a more aggressive disease associated with sustained MAIT cell abnormalities suggests a shorter time of hyperglycemia before the onset thereby lower levels of HbA1c[36].

The strong inverse correlation between GzB production by MAIT cells and the age of the children at the time of onset suggested that MAIT cells could participate to β-cell death. Interestingly, inflammatory cytokines usually produced in inflamed islets during T1D progression (IL1-β, IFN-γ and TNF-α) induce MR1 up-regulation on the human β-cell line, EndoC-βH1 cell (**Fig. 3b**). Moreover, co-culture experiments demonstrated the direct killing of EndoC-βH1 cells[37] by purified MAIT cells from four healthy donors. Cell-sorted MAIT cells were cultured in presence of IL-7, then co-cultured with Endo-βH1 cells pre-incubated with inflammatory cytokines, or not. The data in **Figure 3c-d** show that MAIT cells induced MR1-dependent EndoC-βH1 cell apoptosis (annexin V$^+$ PI$^-$), which was more efficient with Endo-βH1 cells pre-incubated with inflammatory cytokines. During co-cultures MAIT cells were activated (CD25 up-regulation) and degranulated (CD107a$^+$) (**Fig. 3e**). Altogether these data suggest that in the inflamed pancreas during diabetes progression MAIT cells can participate to β-cell destruction.

MAIT cell alterations at different disease stages

To further explore the link between MAIT cell parameters and clinical characteristics, 15 of the children with recent onset T1D were analyzed one year later. Although MAIT cell frequency among T cells remain to a similar level after one year of insulin, both CCR6$^+$ and Bcl-2$^+$ MAIT cell frequencies significantly increased. Conversely the frequencies of CD25$^+$, PD1$^+$, IL-17A$^+$, and to some extent GzB$^+$, MAIT cells decreased to levels observed in the control children **(Fig. 4a)**. This longitudinal analysis strengthened the data obtained in the transversal analysis showing that MAIT cell phenotype was more similar to controls in the children under insulin therapy than at disease onset.

152

MAIT cells as a new biomarker of T1D

Canonical analysis was performed to compare MAIT cell alterations in the three groups of children (controls, recent onset and established T1D). This analysis revealed that MAIT cell parameters were sufficient to discriminate the three groups of children analyzed **(Fig. 4b).** Parameters involved in this discrimination are shown in **supplementary Figure 6.** Moreover, a statistical regression analysis identified four surface markers (CCR6, CD25, PD1, CD56) that define a predictive model for the diagnosis of the disease tested on the ROC curve **(Fig. 4c).** Importantly, we confirmed in another cohort of children from Milano that frequency and phenotype alteration of MAIT cell was observed in recent onset T1D as compared to age-matched control children **(Supplementary Table 3 and supplementary Fig. 7).** However technical difficulties impacting CD56 analysis on these frozen cells did not allow to applying the predictive model.

Finally, to test whether MAIT cell alterations could be detected before the onset of diagnosis, we characterized MAIT cells in adults at risk to develop T1D defined as direct relatives of T1D patients with at least two positive autoantibodies **(Supplementary Table 4)**. As compared to the control group, there were increased frequencies of CD25$^+$ and PD1$^+$ MAIT cells and a trend toward a lower CCR6$^+$ MAIT cell frequency, even though the number of individuals analyzed were limited **(Fig. 4d)**. Altogether our data in patients suggest that MAIT cells represent a new biomarker in T1D and they could play a role in the pathogenesis of T1D. Therefore, we investigated MAIT cells in mouse models, which allow analysis in tissues at different stages of disease development and could be manipulated to determine whether MAIT cells are involved in T1D physiopathology.

MAIT cell characterization in NOD mice

The NOD mouse is the most studied animal model of T1D because it shares many features with the human disease[3,4], thus we investigated whether any of the MAIT cell alterations observed in T1D patients were evident in this model. MAIT cells were characterized, in 10 week-old NOD and C57BL/6 mice, using mouse-MR1 tetramers loaded with the riboflavin derivative 5-OP-RU, whereas control tetramers were loaded with the non-agonist folate derivative Ac-6-FP[20,27,32,38] **(Fig. 5a).** The frequency and absolute number of MAIT cells were lower in NOD than C57BL/6 mice; 3 to 10-fold lower in spleen and pancreatic lymph nodes

(PLN). However MAIT cells were present in pancreatic islets of NOD mice and were more abundant in the ileum of NOD than C57BL/6 mice **(Fig. 5b).** Of note circulating MAIT cells were below detection limit in the blood from NOD mice**.** Mouse MAIT cells can be divided in three subsets, CD4^{+}, CD8^{+} or DN[38] (**Fig. 5c-d**). As previously shown, MAIT cells in peripheral tissues of C57BL/6 mice were mainly DN and expressed CD44 (**Fig. 5d supplementary Fig. 8**), corresponding to functionally mature MAIT cells[32]. In contrast, the proportion of DN MAIT cells was lower in NOD than C57BL/6 mice (**Fig. 5c-d**). Analysis of activation markers on MAIT cells from NOD mice revealed that CD69 was highly expressed in pancreatic islets and ileum, and CD25 was elevated in PLN and islets (**Fig. 5e-f**). While CD69 was also elevated on ileum MAIT cells from C57BL/6 mice, CD25 was not up-regulated in PLN from C57BL/6 mice (**Fig. 5f and supplementary Fig. 9**). Of note CD44 was more expressed on ileal MAIT cells from NOD than C57BL/6 mice. Regarding cytokine production in NOD mice, in all tissues MAIT cells are strong producers of IL-17A and TNF-α, whereas IFN-γ and IL-22 was detected in only few cells (**Fig. 5g-h and supplementary Fig. 10**). Moreover, a majority of MAIT cells in PLN and ileum from NOD mice express CD44 and they produce large amount of cytokines. Interestingly, similar results were obtained for TNF-α, IFN-γ and IL-22 cytokine production in both C57BL/6 and NOD mice (**Fig. 5h and supplementary Fig. 11**). Of note, higher frequency of MAIT cells from NOD produce IL-17, compare to C57BL/6, which could contribute to inflammation and diabetes progression. As in C57BL/6 mice[34,38,39], most MAIT cells in NOD mice express PLZF, ROR-γt and T-bet, transcription factors characteristic of this innate-like T cell lineage[23] (**supplementary Fig. 12**). Altogether these data show that spleen MAIT cells are less frequent and mature in NOD than in C57BL/6 mice, however they express an activated phenotype and produce cytokines in PLN, islets and ileum from NOD mice.

MAIT cell accumulation and dual function during diabetes development in NOD mice

We next analyzed MAIT cells in NOD mice, at three stages of disease development, early stage (6-7 weeks old), pre-diabetic (15-17 weeks old) and mice at the onset of the disease **(Fig. 6a)**. These three stages correspond respectively to mild peri-insulitis characterized by moderate infiltration of inflammatory cells around pancreatic islets, to insulitis associated to partial β-cell destruction and to severe destructive insulitis resulting in insufficient insulin production[4,5] and hyperglycemia. During disease progression, MAIT cell frequency increased

in pancreatic islets and transiently in spleen and ileum (**Fig. 6a**). These data show that disease progression is associated to modification of MAIT cell tissue distribution. Since MAIT cells are effector cells and can migrate to inflamed tissues, we analyzed their migration by transfer experiments. MAIT cells were transferred into congenic NOD mice at two stages of disease development. Interestingly there is a higher recruitment of MAIT cells in the pancreas of 20-25 week old NOD mice than in younger (8-10 week) mice (**Fig. 6 b**). In contrast, MAIT cell recruitment in ileum decreased with aging, supporting the decreased frequency of MAIT cells in this tissue in diabetic NOD mice.

To further explore the function of MAIT cells in T1D, their cytokine production was analyzed in various tissues at the three stages of disease development. For that purpose, MAIT cells were purified by cell-sorter after MR1-tetramer staining, and level of GzB, IFN-γ, IL-17A and IL-22 mRNA was analyzed by RT-qPCR (**Fig. 6c-d)**. Interestingly, in pancreatic islets and ileum, MAIT cell cytokine profiles evolved with disease progression. In islets, MAIT cell production of IFN-γ was detected in diabetic mice, and GzB was already detectable at pre-diabetic stage and further increased in diabetic mice (**Fig. 6c**). Both GzB and IFN-γ from MAIT cells could participate to pancreatic β-cell death[4]. This increased production of IFN-γ and GzB in islets was confirmed at protein levels (**Fig. 6e).** In ileum from NOD mice, T1D development was associated with decreased level of IL-17A and IL-22 mRNA in MAIT cells at the diabetic stage (**Fig. 6d**). Diminished IL-17A and IL-22 production by ileal MAIT cells from diabetic NOD mice was confirmed by intra-cellular staining (**Fig. 6f**). Altogether these results suggest that MAIT cells could play a dual role in NOD mice according to their tissue localization, promoting β-cell death in the pancreas whereas participating in gut mucosa homeostasis.

Gut mucosa alterations during T1D progression in NOD mice

Since ROR-γt is the master transcription factor for IL-17A[40] and is involved in IL-22 production[41,42], we analyzed ROR-γt expression in MAIT cells in the ileum of ROR-γt-GFP NOD mice (**Fig. 7a**). According to the decreased level of IL-17A and IL-22 in diabetic mice, ROR-γt expression was also impacted at the onset of the disease. Decreased IL-17, IL-22 and ROR-γt expression by MAIT cells in diabetic NOD mice prompt us to analyze IL-23 expression, a key cytokine inducing the production of these cytokines. Interestingly, at diabetes onset IL-23 transcript level was decreased in the ileum (**Fig. 7b**), which could contribute to the

decreased IL-17/IL-22 production by MAIT cells. Of note, this defect in cytokine production is associated with significant increased gut permeability, as measured by in vivo FITC-dextran assay (**Fig. 7c**).

To investigate whether gut microbiota could directly impact MAIT cell function, we measured at different stages of disease development the level of bacterial agonist ligand in intestinal content using an in vitro biological assay (**Fig. 7d-g**). Intestinal contents activate purified MAIT cells is a dose dependent manner, as 5-OP-RU positive control (**Fig. 7d-e**). This activation was MR1 specific since it was inhibited by the addition of Ac-6-FP antagonist ligand (**Fig. 7d-f**). MAIT cell activation by intestinal contents from young, pre-diabetic and diabetic NOD mice did not reveal significant modification of MAIT cell ligand concentration (**Fig. 7g**). Altogether, these data suggest that MAIT cell defective IL-17 and IL-22 production might be due to lower IL-23 level in diabetic mice in association to increased gut permeability.

Absence of MAIT cells impacts diabetes development and intestinal homeostasis.

To determine the role of MAIT cells in the pathogenesis of T1D, we generated MR1$^{-/-}$ NOD mice, since MR1 is required for thymic development of MAIT cells[18,32,33,43]. Our analysis was performed on MR1$^{-/-}$ and MR1$^{+/-}$ littermate NOD mice in co-housed condition to exclude possible impact of different gut microbiota on MAIT cell function. As expected MR1$^{-/-}$ NOD mice lacked MAIT cells, whereas there were no significant differences in the frequency of Foxp3^{+} CD4 Treg, iNKT and $\gamma\delta$T cells in the spleen and PLN from both lines (**Fig. 8a and supplementary Fig. 13**). Most interestingly, MR1$^{-/-}$ NOD mice developed exacerbated diabetes compared to their littermate MR1$^{+/-}$ controls indicating a protective role of MAIT cells in T1D development (**Fig. 8b**). Of note, we also observed the protective role of MAIT cells against T1D using multi-low dose streptozotocin treatment, commonly used to induce T1D in C57BL/6 mice[44]. As shown in the **supplementary Fig. 14**, MR1$^{-/-}$ B6-MAIT^{CAST} mice were more susceptible to T1D development than their MR1$^{+/-}$ B6-MAIT^{CAST} littermates. Corroborating incidence results in NOD mice, there was an elevated frequency of anti-islet CD8^{+} T cells specific for islet-specific glucose-6-phosphatase catalytic subunit-related protein (IGRP)[45] and IFN-γ^{+} anti-IGRP CD8 T cells, respectively in the PLN and pancreatic islets, from MR1$^{-/-}$ NOD mice compared to their littermate controls (**Fig. 8c-d**). Since PLN dendritic cells (DC) play a key role in anti-islet T cell priming[46,47], DC phenotype was analyzed in both lines

278 of NOD mice. Supporting increased anti-islet T cell response, CD11c^{+}CD11b^{+}CD103^{+} DC[48–50]

279 frequency was elevated in PLN from MR1^{-/-} NOD mice and these DC expressed higher level of

280 MHC class II molecules and CD86 reflecting their more activated status (**Fig. 8e**). Since gut

281 mucosa integrity controls immune cell activation[44,51,52] and MAIT cells are abundant and

282 activated in this tissue, we explored gut mucosa of MR1^{-/-} NOD mice. The lack of MAIT cells

283 resulted in a significant increased intestinal permeability evaluated by FITC-dextran level in

284 the blood after oral gavage **(Fig. 8f)**. Reduced mRNA expression of occludin and mucin-2

285 confirmed defective gut epithelial cell function and histology analysis showed an abnormal

286 mucus accumulation in goblet cells of MR1^{-/-} NOD mice **(Fig. 8g-h)**. These abnormalities were

287 associated with increased lymphoid cell infiltration in the lamina propria (**Fig. 8i**). Regarding

288 the role of MAIT cells in the control of gut integrity and DC priming in the PLN, significant

289 increased level of bacterial DNA 16S was detected in the PLN of MR1^{-/-} versus control

290 littermates (**Fig. 8j**). Altogether, our data reveal a link between MAIT cells, the gut mucosa

291 and the increased anti-islet T cell responses.

292

293

294 **Discussion**

295 This study reveals MAIT cell alteration in T1D patients as well as in NOD mice. MAIT cell

296 frequency is lower in the peripheral blood of patients compared to healthy children. Such

297 decreased frequency could reflect their migration from the blood to inflamed tissues as

298 described in other inflammatory and autoimmune diseases[24–26,29,53–55] and as supported by

299 their increased frequency and migration in the pancreas of NOD mice during T1D

300 development. Lower frequency of blood MAIT cells could also result from their sustained

301 activation leading to cell exhaustion as indicated by their expression of Bcl-2, CD25 and PD1

302 and by their defective *in vitro* response to Ag specific stimulation, in contrast to their

303 increased cytokines and GzB production upon PMA-ionomycin. Of note MAIT cell defect in

304 T1D might not only be a consequence of diabetes development but also might reflect

305 intrinsic differences. Indeed in NOD mice, as compared to C57BL/6 mice, MAIT cells are less

306 frequent and express a less mature phenotype, based on CD44 expression.

307 Our study in NOD mice points out the different phenotype and function of MAIT cells

308 according to their tissue localization. This heterogeneity of MAIT cells observed in mice

10

might explain the mosaic of MAIT cell populations detected in the blood from control individuals and T1D patients. It would be interesting to further investigate the recirculation of MAIT cells between peripheral tissues and the blood. However study of blood MAIT cells in NOD mice was not performed due to their extremely low frequency.

The analysis of peripheral tissues from NOD mice highlights the role of MAIT cells in two tissues, the pancreas and the gut mucosa. In the pancreas, not only MAIT cell frequency increased with diabetes development but also their production of GzB and IFN-γ, which could participate to the destruction of β-cells[4,5]. Most interestingly, in the youngest children with recent onset T1D, usually associated to a more aggressive disease[35,36], circulating MAIT cells express the highest level of GzB. This parameter has the strongest correlations with clinical characteristics, age at diagnosis and % of HbA1c. Of note, increased GzB production was not observed in other T cell populations (data not shown). Moreover co-culture experiments show that MAIT cells are able to directly kill human β cell line.

In contrast to the pancreas, in the gut mucosa MAIT cells might play a protective role through their production of IL-17A and IL-22, two key cytokines in intestinal homeostasis[41,42,56,57]. The presence of gut alterations as T1D progress in NOD mice underscores the importance of MAIT cells in maintaining gut mucosa homeostasis. Moreover the lack of MAIT cells in MR1^{-/-} NOD mice is associated with a loss of gut integrity shown by FITC-dextran assay, decreased expression of tight junction proteins and abnormal mucus distribution. Absence of MAIT cells in NOD mice favors gut leakiness, associated with translocation of bacteria components, such as 16S bacterial DNA, from the gut to peripheral tissues. The presence of bacterial DNA could promote T1D development through DC activation via TLR receptors in PLN and increased anti-islet pathogenic T cell responses. Altogether, our data support the model in which MAIT cell deficiency aggravates gut mucosa alterations, thereby promoting T1D development. These data are reminiscent of recent reports showing a critical link between the gut mucosa and the development of inflammatory and autoimmune diseases including T1D[44,51,52]. MAIT cells could act as a sensor of environmental changes by responding to alteration of gut mucosa by modulating the host immune system. Their abundance and activation status (CD69, cytokine production) in the gut could explain the prominent regulatory role of MAIT cells in the intestinal mucosa of NOD mice.

340   Overall the present study reveals MAIT cell alteration in T1D patients as well as in NOD mice

341   and highlights the protective role of MAIT cells against diabetes, despite their infiltration in

342   the pancreas of NOD mice and their production of GzB and IFN-γ. These data lead us to

343   propose that MAIT cells are at the crossroad between gut mucosa, inflammation and T1D

344   (**supplementary Fig. 15**). Interestingly, MAIT cell alteration in both patients and mice has

345   been detected before the onset of diabetes, indicating that MAIT cell could represent a new

346   biomarker of T1D development. Moreover, our data suggesting the protective role of MAIT

347   cells in NOD mice at the level of the gut mucosa could pave the way for the development of

348   new therapeutic strategies based on their local triggering in this tissue at early phase of

349   disease development.

Author contributions

OR, JDS, LB, IN performed most of the experiments and data analyses; CT, BK, LC performed experiments; MO and MD participated to experiments with EndoC-β1 cell line; JR, JMC provided mouse MR1 tetramers; OL provided MR1^{-/-} C57BL/6 and B6-MAIT[CAST] mice and

reagents; MB, MP and JB characterized patients and provided human samples; OR, IN, AL wrote the manuscript; JR, JMC, RS and OL provided intellectual input. AL supervised the work.

References

1. Atkinson, M. A., Eisenbarth, G. S. & Michels, A. W. Type 1 diabetes. *Lancet* **383,** 69–82 (2014).

2. Diana, J. *et al.* Crosstalk between neutrophils, B-1a cells and plasmacytoid dendritic cells initiates autoimmune diabetes. *Nat. Med.* **19,** 65–73 (2013).

3. Anderson, M. S. & Bluestone, J. A. The NOD mouse: a model of immune dysregulation. *Annu. Rev. Immunol.* **23,** 447–485 (2005).

4. Lehuen, A., Diana, J., Zaccone, P. & Cooke, A. Immune cell crosstalk in type 1 diabetes. *Nat. Rev. Immunol.* **10,** 501–513 (2010).

5. Bluestone, J. A., Herold, K. & Eisenbarth, G. Genetics, pathogenesis and clinical interventions in type 1 diabetes. *Nature* **464,** 1293–1300 (2010).

6. Wen, L. *et al.* Innate immunity and intestinal microbiota in the development of Type 1 diabetes. *Nature* **455,** 1109–1113 (2008).

7. Markle, J. G. M. *et al.* Sex differences in the gut microbiome drive hormone-dependent regulation of autoimmunity. *Science* **339,** 1084–1088 (2013).

8. Yurkovetskiy, L. *et al.* Gender bias in autoimmunity is influenced by microbiota. *Immunity* **39,** 400–412 (2013).

9. Sun, J. *et al.* Pancreatic β-Cells Limit Autoimmune Diabetes via an Immunoregulatory Antimicrobial Peptide Expressed under the Influence of the Gut Microbiota. *Immunity* **43,** 304–317 (2015).

10. Kostic, A. D. *et al.* The dynamics of the human infant gut microbiome in development and in progression toward type 1 diabetes. *Cell Host Microbe* **17,** 260–273 (2015).

11. Alkanani, A. K. *et al.* Alterations in Intestinal Microbiota Correlate With Susceptibility to Type 1 Diabetes. *Diabetes* **64,** 3510–3520 (2015).

12. Vatanen, T. *et al.* Variation in Microbiome LPS Immunogenicity Contributes to Autoimmunity in Humans. *Cell* **165,** 1551 (2016).

406   13.   Alam, C. *et al.* Inflammatory tendencies and overproduction of IL-17 in the colon of young

407   NOD mice are counteracted with diet change. *Diabetes* **59,** 2237–2246 (2010).

408   14.   Alam, C. *et al.* Effects of a germ-free environment on gut immune regulation and diabetes

409   progression in non-obese diabetic (NOD) mice. *Diabetologia* **54,** 1398–1406 (2011).

410   15.   Bosi, E. *et al.* Increased intestinal permeability precedes clinical onset of type 1 diabetes.

411   *Diabetologia* **49,** 2824–2827 (2006).

412   16.   Sapone, A. *et al.* Zonulin upregulation is associated with increased gut permeability in

413   subjects with type 1 diabetes and their relatives. *Diabetes* **55,** 1443–1449 (2006).

414   17.   Badami, E. *et al.* Defective differentiation of regulatory FoxP3+ T cells by small-intestinal

415   dendritic cells in patients with type 1 diabetes. *Diabetes* **60,** 2120–2124 (2011).

416   18.   Treiner, E. *et al.* Selection of evolutionarily conserved mucosal-associated invariant T cells by

417   MR1. *Nature* **422,** 164–169 (2003).

418   19.   Kjer-Nielsen, L. *et al.* MR1 presents microbial vitamin B metabolites to MAIT cells. *Nature*

419   **491,** 717–723 (2012).

420   20.   Corbett, A. J. *et al.* T-cell activation by transitory neo-antigens derived from distinct microbial

421   pathways. *Nature* **509,** 361–365 (2014).

422   21.   Birkinshaw, R. W., Kjer-Nielsen, L., Eckle, S. B. G., McCluskey, J. & Rossjohn, J. MAITs, MR1

423   and vitamin B metabolites. *Curr. Opin. Immunol.* **26,** 7–13 (2014).

424   22.   Dusseaux, M. *et al.* Human MAIT cells are xenobiotic-resistant, tissue-targeted, CD161hi IL-

425   17-secreting T cells. *Blood* **117,** 1250–1259 (2011).

426   23.   Franciszkiewicz, K. *et al.* MHC class I-related molecule, MR1, and mucosal-associated

427   invariant T cells. *Immunol. Rev.* **272,** 120–138 (2016).

428   24.   Magalhaes, I. *et al.* Mucosal-associated invariant T cell alterations in obese and type 2

429   diabetic patients. *J. Clin. Invest.* **125,** 1752–1762 (2015).

430   25.   Illés, Z., Shimamura, M., Newcombe, J., Oka, N. & Yamamura, T. Accumulation of Valpha7.2-

431   Jalpha33 invariant T cells in human autoimmune inflammatory lesions in the nervous system. *Int.*

432   *Immunol.* **16,** 223–230 (2004).

433   26.   Serriari, N.-E. *et al.* Innate mucosal-associated invariant T (MAIT) cells are activated in

434   inflammatory bowel diseases. *Clin. Exp. Immunol.* **176,** 266–274 (2014).

435   27.   Chen, Z. *et al.* Mucosal-associated invariant T-cell activation and accumulation after in vivo

436   infection depends on microbial riboflavin synthesis and co-stimulatory signals. *Mucosal Immunol.*

437   (2016). doi:10.1038/mi.2016.39

438   28.   Le Bourhis, L. *et al.* MAIT cells detect and efficiently lyse bacterially-infected epithelial cells.

439   *PLoS Pathog.* **9,** e1003681 (2013).

440   29.   Jeffery, H. C. *et al.* Biliary epithelium and liver B cells exposed to bacteria activate

441   intrahepatic MAIT cells through MR1. *J. Hepatol.* **64,** 1118–1127 (2016).

442   30.   Kurioka, A. *et al.* MAIT cells are licensed through granzyme exchange to kill bacterially

443   sensitized targets. *Mucosal Immunol.* **8,** 429–440 (2015).

444   31.   Walker, L. J. *et al.* Human MAIT and CD8αα cells develop from a pool of type-17

445   precommitted CD8+ T cells. *Blood* **119,** 422–433 (2012).

446   32.   Koay, H.-F. *et al.* A three-stage intrathymic development pathway for the mucosal-associated

447   invariant T cell lineage. *Nat. Immunol.* **17,** 1300–1311 (2016).

448   33.   Martin, E. *et al.* Stepwise development of MAIT cells in mouse and human. *PLoS Biol.* **7,** e54

449   (2009).

450   34.   Reantragoon, R. *et al.* Antigen-loaded MR1 tetramers define T cell receptor heterogeneity in

451   mucosal-associated invariant T cells. *J. Exp. Med.* **210,** 2305–2320 (2013).

452   35.   Leete, P. *et al.* Differential Insulitic Profiles Determine the Extent of β-Cell Destruction and

453   the Age at Onset of Type 1 Diabetes. *Diabetes* **65,** 1362–1369 (2016).

454   36.   Komulainen, J. *et al.* Clinical, autoimmune, and genetic characteristics of very young children

455   with type 1 diabetes. Childhood Diabetes in Finland (DiMe) Study Group. *Diabetes Care* **22,** 1950–

456   1955 (1999).

457   37.   Ravassard, P. *et al.* A genetically engineered human pancreatic β cell line exhibiting glucose-

458   inducible insulin secretion. *J. Clin. Invest.* **121,** 3589–3597 (2011).

459   38.   Rahimpour, A. *et al.* Identification of phenotypically and functionally heterogeneous mouse

460   mucosal-associated invariant T cells using MR1 tetramers. *J. Exp. Med.* **212,** 1095–1108 (2015).

461   39.   Cui, Y. *et al.* Mucosal-associated invariant T cell-rich congenic mouse strain allows functional

462   evaluation. *J. Clin. Invest.* **125,** 4171–4185 (2015).

463   40.   Ivanov, I. I. *et al.* The orphan nuclear receptor RORgammat directs the differentiation

464   program of proinflammatory IL-17+ T helper cells. *Cell* **126,** 1121–1133 (2006).

465   41.   Dudakov, J. A., Hanash, A. M. & van den Brink, M. R. M. Interleukin-22: immunobiology and

466   pathology. *Annu. Rev. Immunol.* **33,** 747–785 (2015).

467   42.   Rutz, S., Wang, X. & Ouyang, W. The IL-20 subfamily of cytokines--from host defence to tissue

468   homeostasis. *Nat. Rev. Immunol.* **14,** 783–795 (2014).

469   43.   Seach, N. *et al.* Double positive thymocytes select mucosal-associated invariant T cells. *J.

470   Immunol. Baltim. Md 1950* **191,** 6002–6009 (2013).

471   44.   Costa, F. R. C. *et al.* Gut microbiota translocation to the pancreatic lymph nodes triggers

472   NOD2 activation and contributes to T1D onset. *J. Exp. Med.* **213,** 1223–1239 (2016).

473   45.   Amrani, A. *et al.* Progression of autoimmune diabetes driven by avidity maturation of a T-cell

474   population. *Nature* **406,** 739–742 (2000).

475   46.   Diana, J. *et al.* Viral infection prevents diabetes by inducing regulatory T cells through NKT

476   cell-plasmacytoid dendritic cell interplay. *J. Exp. Med.* **208,** 729–745 (2011).

477   47.   Turley, S., Poirot, L., Hattori, M., Benoist, C. & Mathis, D. Physiological beta cell death triggers

478   priming of self-reactive T cells by dendritic cells in a type-1 diabetes model. *J. Exp. Med.* **198,**

479   1527–1537 (2003).

480   48.   Fujimoto, K. *et al.* A new subset of CD103+CD8alpha+ dendritic cells in the small intestine

481   expresses TLR3, TLR7, and TLR9 and induces Th1 response and CTL activity. *J. Immunol. Baltim. Md*

482   *1950* **186,** 6287–6295 (2011).

483   49.   Cerovic, V., Bain, C. C., Mowat, A. M. & Milling, S. W. F. Intestinal macrophages and dendritic

484   cells: what's the difference? *Trends Immunol.* **35,** 270–277 (2014).

485   50.   Murphy, T. L. *et al.* Transcriptional Control of Dendritic Cell Development. *Annu. Rev.*

486   *Immunol.* **34,** 93–119 (2016).

487   51.   Kawano, Y. *et al.* Colonic Pro-inflammatory Macrophages Cause Insulin Resistance in an

488   Intestinal Ccl2/Ccr2-Dependent Manner. *Cell Metab.* **24,** 295–310 (2016).

489   52.   Garidou, L. *et al.* The Gut Microbiota Regulates Intestinal CD4 T Cells Expressing RORγt and

490   Controls Metabolic Disease. *Cell Metab.* **22,** 100–112 (2015).

491   53.   Cho, Y.-N. *et al.* Mucosal-associated invariant T cell deficiency in systemic lupus

492   erythematosus. *J. Immunol. Baltim. Md 1950* **193,** 3891–3901 (2014).

493   54.   Magalhaes, I., Kiaf, B. & Lehuen, A. iNKT and MAIT Cell Alterations in Diabetes. *Front.*

494   *Immunol.* **6,** 341 (2015).

495   55.   Toubal, A. & Lehuen, A. Lights on MAIT cells, a new immune player in liver diseases. *J.*

496   *Hepatol.* **64,** 1008–1010 (2016).

497   56.   Maxwell, J. R. *et al.* Differential Roles for Interleukin-23 and Interleukin-17 in Intestinal

498   Immunoregulation. *Immunity* **43,** 739–750 (2015).

499   57.   Lee, J. S. *et al.* Interleukin-23-Independent IL-17 Production Regulates Intestinal Epithelial

500   Permeability. *Immunity* **43,** 727–738 (2015).

501   58.   Mahon, J. L. *et al.* The TrialNet Natural History Study of the Development of Type 1 Diabetes:

502   objectives, design, and initial results. *Pediatr. Diabetes* **10,** 97–104 (2009).

503   59.   TrialNet - Information for Patients. Available at:

504   https://www.diabetestrialnet.org/PathwayToPrevention/. (Accessed: 25th January 2017)

505   60.   Lochner, M. *et al.* In vivo equilibrium of proinflammatory IL-17+ and regulatory IL-10+ Foxp3+

506   RORgamma t+ T cells. *J. Exp. Med.* **205,** 1381–1393 (2008).

507   61.   Pickard, J. M. *et al.* Rapid fucosylation of intestinal epithelium sustains host-commensal

508   symbiosis in sickness. *Nature* **514,** 638–641 (2014).

509

Online Methods

Human samples. Peripheral blood samples were obtained from control children and from T1D children admitted in the Pediatric Endocrinology department of Necker hospital, Paris, France at T1D onset (i.e. within 10 days from first insulin injection), or with established disease. All control children, were children presenting at the hospital for growth retardation, short stature or precocious puberty. None of them had any other medical conditions or history of autoimmune disease. Patients with growth retardation or short stature were admitted for a growth hormone stimulation test. All of them were previously screened for coeliac disease or autoimmune thyroiditis that can be an etiology of short stature. This screening was negative for all patients. All of these "control" children were diagnosed with idiopathic growth hormone deficiency or idiopathic short stature. Patients with precocious puberty didn't have either any story of autoimmune disease. They were admitted for a gonadotropin-releasing hormone stimulation test and were diagnosed with idiopathic central precocious puberty. As reported in the method section, all "control" patients were screened for T1D related antibodies that were negative. Non-inclusion clinical following parameters contain: infection during the admission and associated other autoimmune diseases. The Ethics Committee (Comité de protection des personnes (CPP) Ile-de-France) approved the clinical investigations and written informed consent was obtained from all the parents. For the Milan cohort, peripheral blood from healthy control subjects and patients at T1D onset (i.e., within 10 days from first insulin injection) were collected. The study was approved by the San Raffaele Hospital Ethic Committee (protocol: DRI-003). At risk subjects were enrolled in the Type 1 Diabetes TrialNet Pathway to Prevention Trial (TN01 trial, former TrialNet Natural History Study)[58,59] . The overall objective of this study is to perform baseline and repeated assessments over time of the immunologic and metabolic status of individuals who are at risk for T1D (first/second degree relatives of patients with T1D). The study was approved by the San Raffaele Hospital Ethics Committee (protocol: NHPROTOCOL32803 TN01). Our local study was approved by the TrialNet Ancillary Studies Subcommittee. All subjects included in this study signed the informed consent prior to blood donation.

Mice. MR1-/+ NOD mice was generated by backcrosses (>15 times) of MR1^{-/-} C57BL/6J[18,33] on the NOD background, 17 insulin-dependent diabetes (Idd) loci associated with

susceptibility to T1D have been checked on all chromosomes. MR1^{-/-} NOD mice were generated by intercross of MR1^{-/+} NOD mice and the analyses were performed with MR1^{-/-} and MR1^{-/+} NOD littermates kept in co-housed cages. Transgenic ROR-γt-GFP NOD mouse was generated by microinjection of ROR-γt-GFP BAC construct[60] into NOD embryos. B6-MAIT[CAST] mice were provided by O. Lantz[39]. All mice were bred under specific pathogen-free conditions and the study was performed on females, except the steptozotocin experiments. NOD mice were tested weekly (daily in steptozotocin experiments) and considered diabetic after two consecutive positive urine glucose tests (DIABUR-TEST 5000, Roche), confirmed by a glycemia > 200 mg/Dl (ACCU-CHEK, Roche). This study was approved by the ethics committee on animal experimentation CEEA 34 (APAFIS N°2015102016444419).

Cell preparations. Human peripheral blood mono-nucleated cells (PBMC) of patients from Necker Hospital were isolated from fresh blood samples by Ficoll-Paque (Leucosep) or samples from San Raffaele hospital were defrosted in RPMI with 10% FCS (Fetal Cow Serum). Mouse cells were prepared from different tissues as described below. For Pancreatic islets isolation, mice were sacrificed and pancreas was perfused with 3 mL of a collagenase P solution (0.8 mg/mL, Roche), which was then isolated and set free from surrounding tissues and lymph nodes. Digestion of the pancreas was performed at 37°C for 10 min and was stopped by adding large volume of cold 5% FCS RPMI before extensive washes. Pancreatic islets were then purified on a Ficoll discontinuous gradient. For immunofluorescence analysis, islets were dissociated with a non-enzymatic cell-dissociation solution (Sigma). For Intestine cell isolation, Miltenyi Lamina Propria Dissociation Kit for mouse was used to prepare epithelial and lamina propria cells. Mice were sacrificed and intestine was removed from mice. Intestine was cleared of feces, fat tissue and Peyer's patches with HBSS without Ca^{2+} and Mg^{2+} containing 10 mM HEPES solution. After passage through 100 μm filter, the cell suspension was subjected to Percoll (GE Healthcare) density gradient of 40% and 80% and the interface between the layers containing lamina propria lymphocytes were collected and suspended in PBS containing 2% FCS and 0.1% sodium azide. For the preparation of mouse dendritic cells from lymph nodes and spleen, mice were sacrificed and organ were cut in small pieces and then digested at 37°C for 30 min with 2 mL of collagenase D (1.0

mg/mL, Roche) solution. Digestion was stopped by adding a large volume of cold 5% FCS
RPMI, and cells were washed and filtered on cell strainer (40 μm, BD Falcon) before staining.

Flow cytometry and antibodies. Cells were stained in PBS containing 5% FCS and 0.1%
sodium azide. For human PBMC the following antibodies were used: CD3 (OKT3), CD4
(OKT4), Vα7.2 (3C10), CD161 (HP-3G10), CCR6 (G034E3), CD56 (HCD56), CD69 (FN50), Bcl-2
(100), IFN-γ (4S B3), IL-17A (BL168), TNF-α (MAb11) and MR1 (26.5) mAbs from BioLegend;
CD8 (SK1), PD1 (MIH4), CD25 (M-A251), IL-4 (8D4-8), granzyme B (GB11) mAbs and CD107a
(HYA3) from BD Biosciences; CD3 (REA), CD161 (REA) mAbs from Miltenyi and CD4 (RPA-T4)
mAb from eBiosciences. According to the PBCM number obtained from each patient, surface
staining was always performed, and when possible due to the number of PBMC
intracytoplasmic staining of cytokines and GzB after PMA-ionomycin stimulation was
analyzed, and then PBMC bcl-2 expression was analyzed by intracytoplasmic staining
(without stimulation). Data acquisition was performed using BD Biosciences LSR-Fortessa
cytometer or FACS ARIA III cytometer for cells from patients from Necker hospital and
Beckman Coulter Gallios for cells from patients from San Raffaele hospital.

Staining of mouse cells was performed with the following antibodies: TCRβ (H57), TCR-
γδ (GL3), CD45 (30F11), CD8α (53–6.7), CD103 (M290), CD44 (IM7), I-Ak (10-3.6CD45), CD86
(GL1), IL-17A (TC11-18H10) and IFN-γ (XMG1.2) mAbs, were from BD Biosciences; CD19
(6D5), CD4 (GK1.5), CD11b (M1/70), PLZF (9E12), T-bet (4B10), CD25(PC61), CD69 (HI-2F3),
CD304 (3E12), and CXCR3 (SA011F11) mAbs, were from Biolegend; CD11c (N418), CD170
(1RNM44N), F4/80 (BM8), ROR-γt (B2D) and FOXP3 (FJK-16s) mAbs were from eBioscience.
Alpha-Galactosylceramide-CD1d tetramer was prepared by the laboratory and coupled to
streptavidin-BV421 (Biolegend). NRP-V7 tetramer (IGRP206-214 (KYNKANVFL) reactive T cell)
and TUM tetramer (TUM (KYQAVTTTL) reactive T cell, were provided by the National
Institutes of Health tetramer core facility. Biotinylated mouse MR1 tetramers loaded with
the active ligand (5-OP-RU) were used to specifically identify MAIT cells and biotinylated
MR1 tetramers loaded with the non-activating ligand 6-formyl-pterin (6-FP) were used as a
negative control. MR1 tetramers were coupled to streptavidin-PE (BD Biosciences) or
Streptavidin-BV421 (Biolegend) and cells were stained with tetramers for 45 min at RT
before surface staining with mAbs. Data acquisition was performed using a BD Biosciences

602   LSRFortessa or FACS-ARIA III cytometer. Flow cytometric analyses were performed with the

603   FlowJo analysis software V10.1 (Tree Star) and the Spice software V5.3 was used for studying

604   the multiparametric combination of cellular staining.

605

606   **In vitro cell stimulation**. For ligand stimulation of human MAIT cells, 5-OP-RU solution was

607   obtained after incubating 1 molar equivalent of 5-A-RU with 2 molar equivalent of

608   methylglyoxal (Sigma-Aldrich). Co-culture of Hela, expressing MR1 molecules, and PBMC in

609   media containing RPMI supplemented with 10% FCS were done to analyze MAIT cell

610   activation from both controls and recent onset T1D children in presence of MAIT cell ligand

611   (5-OP-RU). Briefly, cells were plated at final concentration of 1 x 10^6 PBMC/mL and 1 x 10^6

612   Hela/mL (1:1 ratio). In these cultures, MAIT cells were stimulated O.N. by the addition of

613   their agonist ligand (5-OP-RU) at various concentration (0-5 nmol/L), in presence of blocking

614   anti-MR1 (26.5 mAb) or not. Then, MAIT were stained with appropriate antibodies and cell

615   surface activation markers were analyzed by flow cytometry.

616

617   **Intra-cellular staining.** For human Bcl-2 and mouse transcription factor staining, after

618   surface staining lymphocytes were resuspended in fixation/permeabilization buffer (Foxp3

619   staining kit from eBioscience) and incubated at 4°C in the dark then, cells were washed with

620   PERM Wash buffer (eBioscience) and labeled with appropriate mAbs. For cytokine and

621   granzyme B analysis of human MAIT cells, PBMC obtained from fresh samples, were

622   analyzed after stimulation for 6 h at 37°C in RPMI medium supplemented with 10% FCS with

623   PMA (25 ng/ml) and ionomycin (1 µg/ml), in the presence of Brefeldin A (10 µg/ml). For

624   cytokine staining of mouse lymphocytes, cells were stimulated with PMA (10 ng/mL) and

625   ionomycine (1 µg/mL) in the presence of Brefeldin A (10 µg/mL) for 4 h at 37°C (all reagents

626   from Sigma-Aldrich) or cells were stimulated in vivo by i.v. injection of flagellin (FLA-PA) at 3

627   µg/mouse 2 h before analysis, as previously described[61]. After surface staining, cells were

628   fixed and permeabilized with Cytofix/Cytoperm kit (BD Biosciences) washed and incubated

629   at 4°C in the dark for 30 min with anti-cytokines.

630

β-cell death induction by MAIT cells. EndoC-βH1[37] was provided and cultured by R. Scharfmann laboratory. EndoC-βH1 were platted at final concentration of 0.35 x 10^6 cells/mL during 24 h in specifically formulated DMEM media containing 5.6 mM glucose, 2% BSA fraction V (Roche diagnostics), 50 µM 2-mercaptoethanol, 5 µg/ml transferrin (Sigma-Aldrich), 6.7 ng/ml selenite (Sigma-Aldrich), 100 U/mL penicillin, 100 µg/mL streptomycin. One day later, when indicated cytokines (TNF-α 1.100 U/mL, IL-1β 1.000 U/mL, IFN-γ 2.000 U/mL) were added in EndoC-βH1 cultures for 24 h. In parallel MAIT cells from donors were purified by negative isolation with Dynabeads Goat anti-Mouse IgG (Invitrogen), then stained with appropriate antibodies and sorted by FACS-ARIA. After sorting, MAIT cells were cultured in complete medium containing RPMI supplemented with 10% FCS, 1% penicillin/ streptomycin, 1% HEPES and supplemented with 25 ng/mL recombinant human IL-7 (R&D Systems) for 48 h. Then, MAIT cells were added to EndoC-βH1 cultures at 1:1 ratio and cultured 24 h in presence of different concentrations of 5-OP-RU. Blocking MR1 mAb (26.5) was added when indicated. MAIT cells were recovered in the supernatants and analyzed by flow cytometry for their surface expression of CD25 and CD107a. Adherent EndoC-βH1 cells were harvested and stained with APC Annexin V Apoptosis Detection Kit with PI (Biolegend) according to the manufacturer's instruction. Cells were analyzed using LSRFortessa cytometer.

Isolation of RNA and real-time reverse PCR analysis. Mouse cells were lysed in RLT buffer with 1% β-mercaptoethanol, and mRNA was purified from lysed cells using RNeasy Mini Kit (Qiagen). cDNA was produced using the Superscript III reverse transcriptase (Invitrogen). Quantitative-PCR analysis was performed with SYBR Green (Roche) and analyzed with a LightCycler 480 (Roche). The relative expression was calculated using the $2^{-\Delta\Delta Ct}$ method and normalized to the expression of the housekeeping gene GAPDH. The stability of GAPDH expression was confirmed by comparison with HPRT mRNA. The primers used for qPCR are described in **Supplementary Table 5**.

MAIT cell transfer experiment. CD45.2 MAIT cells were obtained from 9-10 week-old Vα19 transgenic Cα-/- NOD mice. T cells were isolated from splenocytes, MLNs and PLNs by

661 depleting B cells, monocytes/macrophages, NK cells, dendritic cells, erythrocytes, and

662 granulocytes using Dynabeads Untouched Mouse T Cells kit (Invitrogen). These cells were

663 injected i.v. (4 x 10^6 cells/mouse) into CD45.1 NOD females and analyzed several days later

664 as indicated.

665

666 **MAIT cell ligands in intestinal content.** WT3-MR1+ cell line, provided by O. Lantz, was used

667 to detect 5-OP-RU MAIT cells ligand from intestinal contents. Two hours before the

668 experiment, WT3-MR1+ cells were coated onto a 96-flat-well plate at final concentration of

669 0.5 x 10^6 cells/mL in media containing DMEM Glutamax 10% FBS, HEPES 1M, sodium

670 pyruvate 100 mM, NeAA 1% and 1% penicillin/streptomycin. Intestinal content from colons

671 were recovered, weighed and resuspended in PBS. Fecal supernatants were centrifuged at

672 14,000 rpm, 5 min, at 4°C and passed through a 0.22 µM filter. Supernatants were tested at

673 final concentration of 0.7 mg intestinal content/mL. Serial dilutions of 5-OP-RU were used as

674 positive controls and acetyl-6-FP was added to determine MR1-specific activation. MAIT cells

675 from the spleen of Vα19 transgenic Cα-/- mice were purified by negative isolation with

676 Dynabeads Untouched Mouse T Cells kit (Invitrogen) and co-cultured O.N. with WT3-MR1+

677 cells at final concentration of 5 x 10^5 MAIT cells/mL. One day after, MAIT cells were stained

678 with appropriate antibodies and activation was analyzed by flow cytometry.

679

680 **Anti-islet T cell response.** Cells from mouse pancreatic islets were recovered and then

681 cultured for 7 days in RPMI medium containing 10% FCS, 1% penicillin/ streptomycin and 25

682 U/mL of human rIL-2. To evaluate peptide-specific reactive T cells, single cell suspensions

683 from islet culture were stimulated for 5 h with IGRP206-214 peptide (the last 4 h in presence

684 of Brefeldin A) and stained with CD45, CD19, TCRβ, CD8 and IFN-γ mAbs.

685

686 **In vivo analysis of intestinal permeability.** Intestinal permeability was determined in MR1-/-

687 and MR1+/- NOD mice by measuring the level of FITC-dextran in the blood. Briefly, mice

688 were water-starved overnight and in the morning, FITC-dextran (40 kDa; Sigma) was

689 administered by oral gavages (44 mg/100 g body weight). Blood was collected 4 h later and

690 centrifuged at 3000 g for 20 min at 4°C. Plasma (50 µL) was diluted volume to volume with

691 PBS to determine fluorescence using a SPARK 10M (TECAN). The concentration was

692 determined using FITC-dextran dilutions.

693

694 **Alcian blue staining and analysis.** Intestinal sections (1 cm in length) of ileum from mice

695 were collected and immediately fixed in 4% paraformaldehyde PBS. Paraffin-embedded

696 sections from ileum were cut into 4 µm slices and stained with Alcian blue periodic acid

697 using standard techniques. Slices were visualized under a light microscope (Leica) and mean

698 intensity of staining were evaluated with the software inForm 2.0.2 and image J.

699

700 **DNA extraction and 16S rRNA gene.** PLN were recovered from 15-20 week-old MR1-/- and

701 MR1+/- NOD mice and DNA extraction was performed using DNeasy Blood and tissue Kit

702 (QIAGEN) following the manufacturer's instructions. Quantitative-PCR analysis was

703 performed with SYBR Green (Roche) and analyzed with a LightCycler 480 (Roche). The

704 relative expression was calculated using the $2^{-\Delta\Delta Ct}$ methods and normalized to the expression

705 of the housekeeping gene GAPDH. The primers used for qPCR are described in

706 **Supplementary Table 5**. The PCR products were sequenced to confirm their bacterial origins.

707

708 **Statistical analysis.** For human studies, statistical tests between two groups were performed

709 using two-tailed Mann-Whitney test and signed-rank Wilcoxon test with Graph Pad Prism.

710 The Kruskal-Wallis test followed by the Wilcoxon rank sum and the Spearman correlation

711 test was applied for all the correlation analysis with Software R. Corrections for multiple

712 testing had been performed on the human results when we compared flow cytometry data

713 between the three groups (the children with recent onset T1D, children with established T1D

714 and control children); Correction have well been applied after using the signed-rank

715 Wilcoxon test with an adjustment of the p-value with the Holm method to take into account

716 the fact that multiple testing have been performed. A factorial discriminant analysis was

717 performed using the XLSTAT 2016 Software. A logistic regression model was fitted with the

718 PROC CANDISC software (SAS version p.3) then a backward elimination procedure was

719 applied. Prognostic validity of the model was evaluated by the receiver operating

720 characteristic (ROC) curve analysis and measured using the area under the ROC curve (AUC).

721 Statistical analyses were performed using the GraphPad Prism software version 5.00.288 and

722 the R software version 3.2.3. For mouse studies, statistical analysis was performed with

723 Prism software (Graph Pad) using nonparametric tests two-tailed Mann-Whitney or

724 Student's t-test, as appropriate. Diabetes incidence was plotted according to the Kaplan–

725 Meier method and statistical differences between groups were analyzed using the Gehan-

726 Breslow-Wilcoxon test or the log-rank test. P values were considered statistically significant

727 (*P<0.05, **P<0.01, ***P<0.001).

Figure 1. Frequency and phenotype alterations of blood MAIT cells from T1D children.
MAIT cells were analyzed in blood from children with recent onset T1D (n=41), children with established T1D (n=23), as compared with control children (n=22). **(a)** Representative staining of MAIT cells and MAIT cell frequency among T lymphocytes. **(b)** Representative staining and frequency of MAIT cells expressing different cell surface molecules (CCR6, CD56, CD69, CD25, PD1) and intracellular Bcl-2. P values were determined by Kruskal-Wallis test followed by the Wilcoxon rank sum test adjusted with the Holm method. **(c)** Multi-parametric analysis of the frequency of MAIT cells expressing the different combination of the five surface molecules: CCR6, CD56, CD25, CD69 and PD1. Threshold for representation is cell frequency >0.36% of MAIT cells.

Figure 2. Functional alterations of blood MAIT cells from T1D children. MAIT cells were analyzed in blood from children with recent onset T1D (n=25) and children with established T1D (n=18), as compared with control children (n=18). **(a)** Representative intracellular staining of MAIT cells for cytokines and GzB after PMA/ionomycin stimulation and graphs showing the frequency of MAIT cells producing cytokines and GzB. P values were determined by Kruskal-Wallis test followed by the Wilcoxon rank sum test adjusted with the Holm method. **(b)** Multi-parametric analysis of the frequency of MAIT cells expressing the different combination of the five intracellular molecules: GzB, IFN-γ, TNF-α, IL-17 and IL-4. Threshold for representation is cell frequency >0.36% of MAIT cells. Note that data for IL-4 are not shown because IL-4 is expressed with other cytokines and the frequency of each MAIT cell population expressing IL-4 is >0.36%. **(c)** Frequencies of CD69^{+} and CD25^{+}CD69^{+} MAIT cells from children controls (n=6) and children with recent onset T1D (n=7) after ON stimulation with 5-OP-RU at various concentrations (0 to 5 nmol/L). Blocking MR1 mAb was added when indicated. P values were determined by Mann-Whitney test.

Figure 3. Cytotoxic function of MAIT cells on human β cell line. (a) Correlation between the age of children with recent onset T1D (n=25) at diagnosis, HbA1c level and the frequency of blood MAIT cells expressing GzB after PMA/Ionomycin stimulation. P values were determined by Spearman test. **(b)** EndoC-βH1 cells were cultured O.N. with or without cytokines. Cells were stained to analyze MR1 cell surface expression by flow cytometry (n=4) or directly lysated to analyze the relative quantity of MR1 mRNA by RT q-PCR (n=7). For MR1

cell surface expression MFI ± SEM was indicated for each groups and for q-PCR, statistical analysis was performed by two-tailed Mann Whitney test, P-value was indicated on graph and bar represent mean ± SEM. **(c-e)** Induction of EndoC-βH1 cell apoptosis by MAIT cells in co-culture in presence of MAIT cell ligand (5-OP-RU). MAIT cells from healthy donors were sorted and cultured with IL-7 during 48h. EndoC-βH1 cells were cultured with or without cytokines during 24h. Then, MAIT cells and EndoC-βH1 cells were co-cultured for 24h at 1:1 ratio with different doses of 5-OP-RU. **(c)** Representative FACS plots of **(d)** EndoC-βH1 apoptosis by MAIT cells at different doses of 5-OP-RU [0-1000 nmol/L] (n=4). Blocking MR1 mAb was added when indicated. Statistical analysis were performed by two-tailed Mann Whitney test, P-values were indicated on each graph and bar represent mean ± SEM. **(e)** Activation and degranulation of MAIT cells in presence or not of ligand and anti-MR1 (n=2).

Figure 4. MAIT cell characteristics in patients at different disease stages. (a) MAIT cell staining of surface and intracellular molecules performed with PBMC from fifteen children with recent onset T1D at the time of diagnosis (on the left) and around one year after diabetes onset (on the right). P values were determined by Signed-rank Wilcoxon Test. **(b)** Factorial discriminant analysis based on the expression of surface and intracellular molecules by MAIT cells from the children with recent onset T1D (n=20), the children with established T1D (n=15) and the children controls (n=18). **(c)** ROC Curve of the predictive model defining the T1D phenotype. **(d)** FACS Analysis of MAIT cell frequency among T lymphocytes and frequency of MAIT cells expressing different cell surface molecules from frozen PBMC of adult controls (n=11) and adult at risk T1D donors with at least two autoantibodies (n=11). P values were determined by Mann-Whitney test.

Figure 5. Characterization of MAIT cells in NOD and C57BL/6 mice. MAIT cells were identified using mouse MR1-5-OP-RU tetramer and MR1-Ac-6-FP tetramer was used as control. MAIT cells are defined as positive MR1 tetramer (5-OP-RU) and low TCRβ staining. Flow cytometric analysis of spleen, pancreatic lymph nodes (PLN), pancreatic islets and ileum from C57BL/6 and NOD mice at 9-12 weeks of age. **(a)** Representative dot plots of MAIT cell staining and **(b)** frequencies and absolute numbers of MAIT cells among TCRβ+ leucocytes .P values were determined by two-tailed Mann-Whitney test (statistical analysis between tissues from NOD mice; C57BL/6 analyses are not shown). **(c)** Representative dot

plots of CD4 and CD8 expression by MAIT cells in NOD mice and (**d**) graphs showing the proportion of MAIT cell subsets in tissues from C57BL/6 and NOD mice. Data correspond to 8 mice from three independent experiments. Bar represent mean ± SEM. (**e**) Representative histograms and (**f**) graphs showing CD69, CD25 and CD44 expression on MAIT cells from NOD mice (white) and C57BL/6 (black). P values were determined by two-tailed Mann-Whitney test (statistical analysis between tissues from NOD mice; C57BL/6 analyses are not shown). (**g**) Representative dot plots and (**h**) graphs showing intracellular cytokine (IFN-γ, TNF-α, IL-17A and IL-22) staining of MAIT cells in 10 week-old NOD mice (white) and C57BL/6 mice (black), after PMA/ionomycin stimulation.

Figure 6. MAIT cell frequencies and function during diabetes development. (a) MAIT cell frequency in different tissues from NOD mice at three stages of disease development (6 weeks, 16 weeks, and diabetic). For each tissue at least 6 mice per group from five independent experiments were analyzed. Statistics were performed with two tailed Mann-Whitney test. **(b)** Purified MAIT cells from CD45.2 Vα19 transgenic Cα-/- NOD mice were transferred (i.v.) into CD45.1 NOD mice at 8-10 weeks of age or at 22-25 weeks of age (4.5 10^6 cells/mice). At day 5 after transfer, mice were sacrificed and islets and ileum were analyzed. Graphs and representative plots of the frequency and the absolute number of transferred MAIT cells are shown. **(c-d)** Graphs showing the relative quantity of (c) GzB, IFN-γ transcripts in MAIT cells from pancreatic islets and (d) IL-22 and IL-17A transcripts in MAIT cells from ileum at three stages of disease development. Each symbol represents a pool of two mice and data were obtained in two independent experiments. Bars represent mean ± SEM. **(e-f)** Cytokine intracellular staining after in vitro PMA/ionomycin stimulation (e) or in vivo flagellin stimulation (f) of MAIT cells and conventional αβT cells from pre-diabetic (17 weeks) and diabetic mice; (e) GzB and IFN-γ for islets and (f) IL-17A and IL-22 for ileum. Dot plots are representative of two independent experiments, with a total of 6 mice per group.

Figure 7. Gut mucosa alterations during T1D progression in NOD mice. (a) Representative dot plots of RORγt–GFP expression by MAIT cells; representative histogram and graph showing MFI of RORγt–GFP^{+} MAIT cells at three stages of disease development. Data were pooled from two independent experiments. **(b)** Cells of ileal tissue from NOD mice were obtained and analyzed by RT-qPCR at two stages of the disease (10 weeks and diabetic
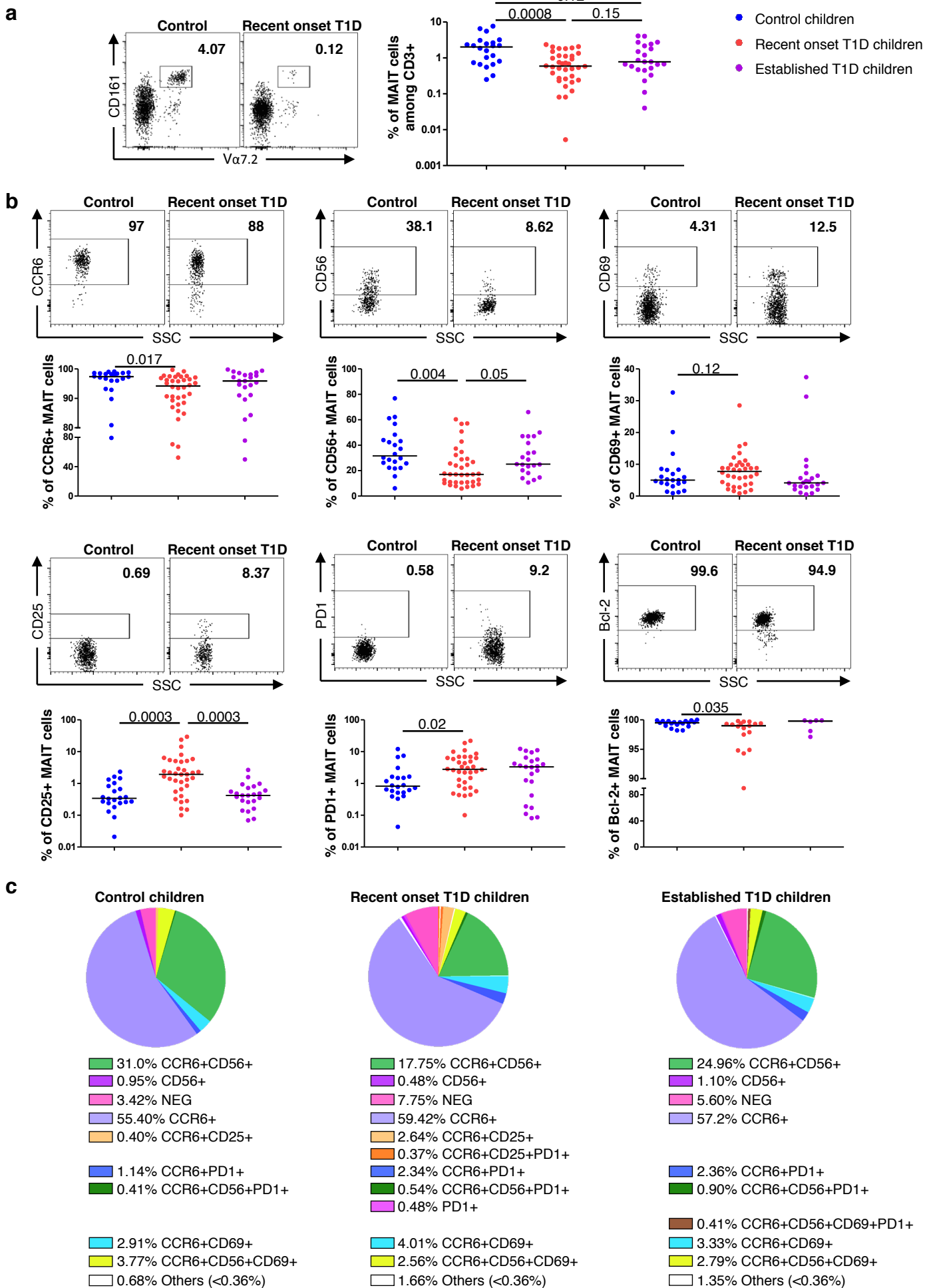
mice); the relative quantity of IL-23 transcript is shown. Data are pooled from two independent experiments. **(c)** Intestinal gut permeability was measured by in vivo FITC-dextran assay in NOD mice at two stages of the disease (10 weeks and diabetic). Data are representative of three independent experiments**. (d-e)** Representative FACS plots and dose response of MAIT cell activation after in presence of WT3- MR1, with different doses of 5-OP-RU ligand and in presence or absence of acetyl-6-FP inhibitor ligand at 10μM. **(d-f)** MAIT cells were activated by fecal supernatants in an MR1-dependent manner. The dose response of MAIT cells activation with different concentrations of fecal supernatants in presence or absence of acetyl-6-FP inhibitor ligand (n=16) is shown. **(g)** Activation of purified MAIT cells by fecal supernatant from NOD mice at different stages of disease development. Data were pooled from three independent experiments. All statistical analyses were performed by two-tailed Mann Whitney test, P-value were indicated on each graph and bar represent mean ± SEM.

Figure 8. MAIT cell deficiency exacerbates diabetes development and alters gut mucosa integrity. All analyses were performed on co-housed MR1$^{-/-}$ and MR1$^{+/-}$ NOD female littermates. **(a)** Representive dot plots of T cell staining with MR1-5-OP-RU and CD1d-α-Galactosyl Ceramide tetramers of splenic cells, gated on αβT cells. Numbers indicate the percentage of MAIT and iNKT cells among TCRβ cells. **(b)** Diabetes incidence of MR1$^{-/-}$ and MR1$^{+/-}$ mice (n=30 and 32 respectively); P values were determined by Gehan-Breslow-Wilcoxon test. **(c)** Representative dot plots and graphs showing percentage of IGRP$_{206-214}$ tetramer positive cells among TCRβ^{+} and CD8^{+} T cells. **(d)** Frequency of IFN-γ$^{.}$ IGRP$_{206-214}$ specific CD8 T cells from pancreatic islets after culture. **(e)** Analysis of CD11c^{+}CD11b^{+}CD103^{+} dendritic cells from ileum, mesenteric (MLN) and pancreatic lymph nodes (PLN). Representative flow cytometry dots showing the gating strategy, MHC class II staining, and graphs showing the absolute numbers of this DC subset, the frequencies and absolute numbers of this DC subset expressing CD86 and MHC class II. **(f)** Intestinal permeability measured by FITC-dextran assay. **(g)** Occludin, mucin-2 and claudin-4 mRNA levels in epithelial cells from ileum. **(h)** Representative photographs of Alcian blue staining of ileum section and graph showing the mean intensity of the staining in Goblet cells. **(i)** Absolute numbers of lymphocytes infiltrating lamina propria. **(j)** DNA from PLN was extracted and then the relative quantity of 16S bacterial DNA was analyzed by qPCR. For graphs a and c-j,
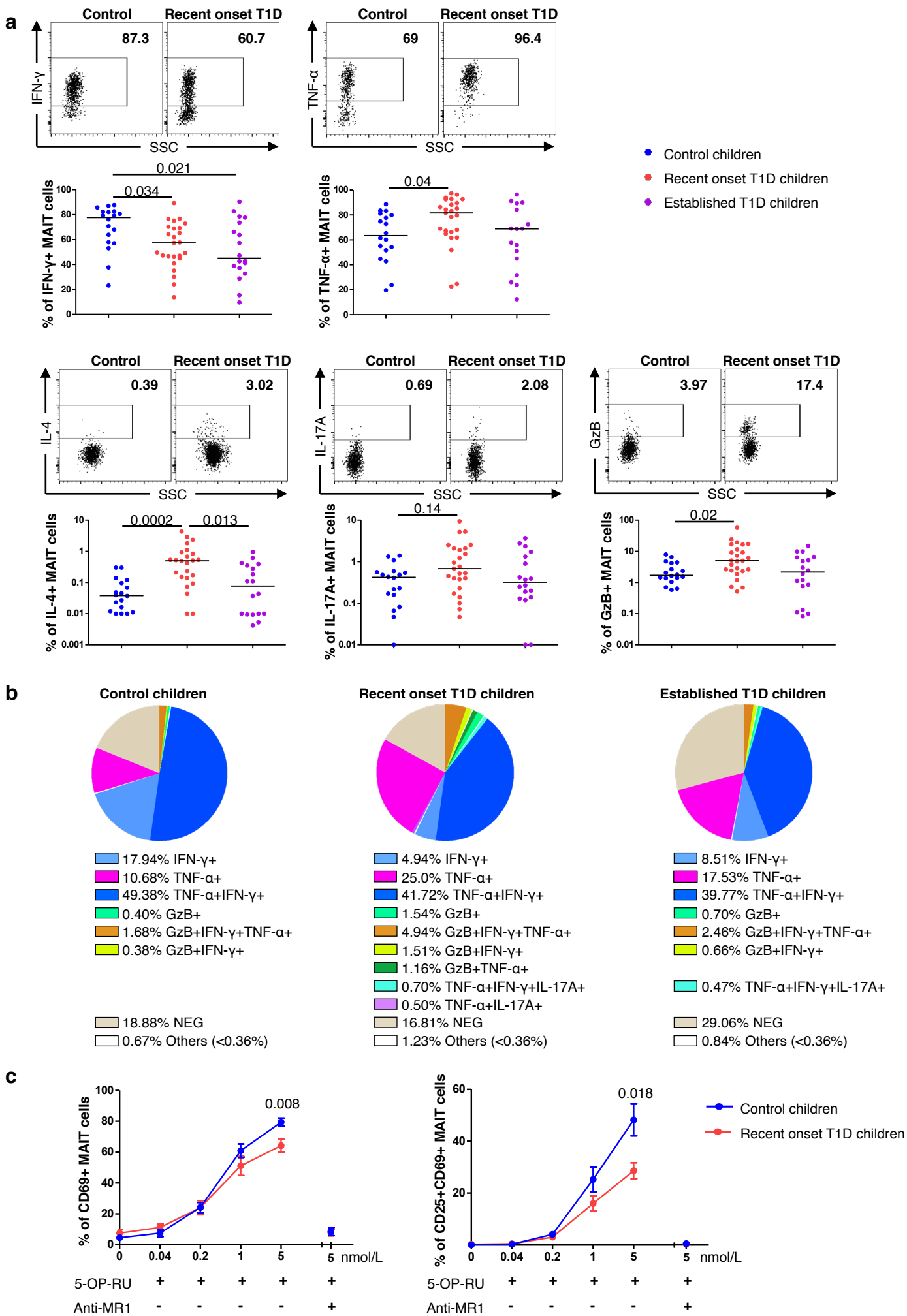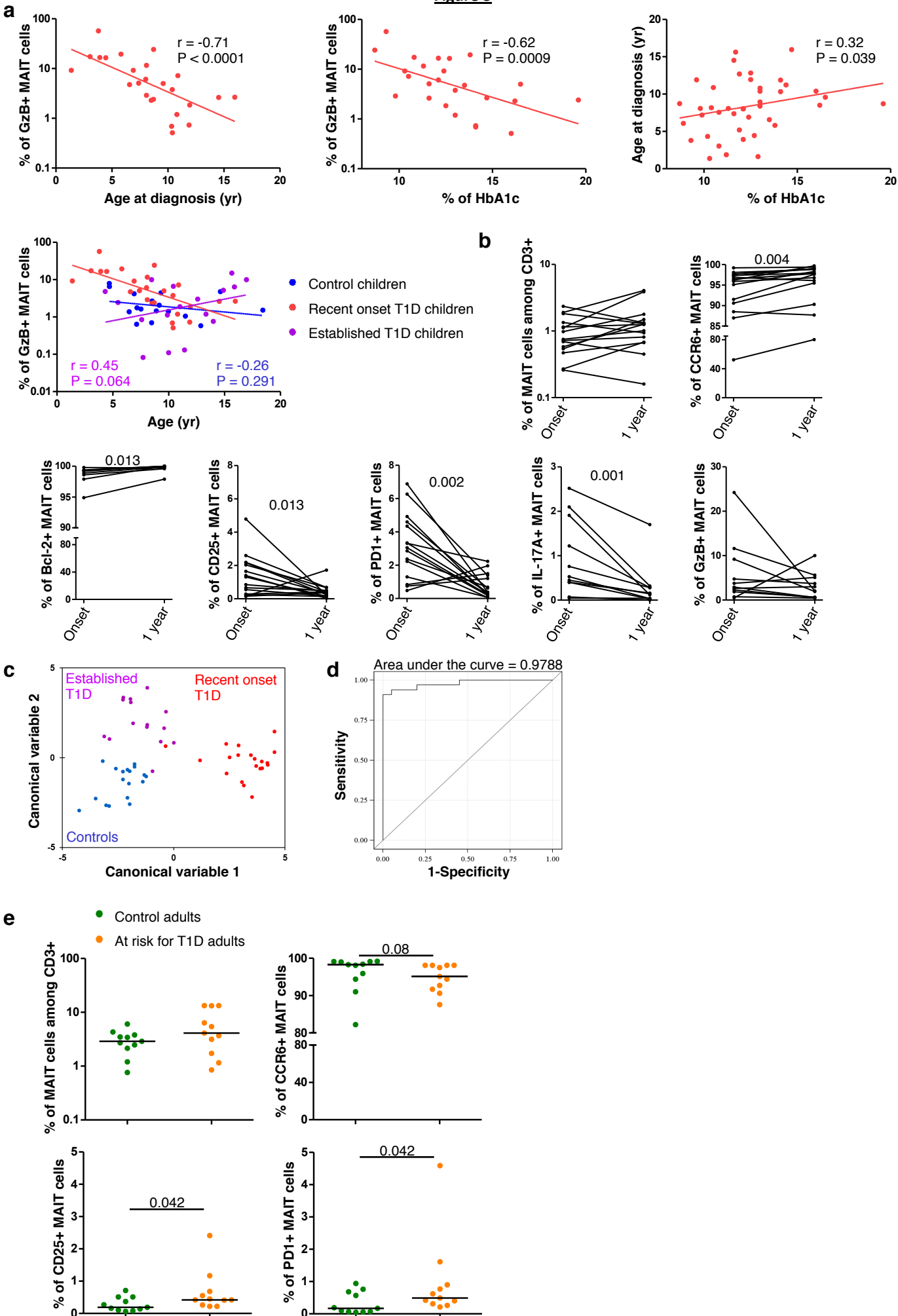
analyses were performed on 15 week-old mice, each point represents an individual mouse, data were pooled from two or three independent experiments, P values were determined by Mann-Whitney test. Bars represent mean ± SEM.
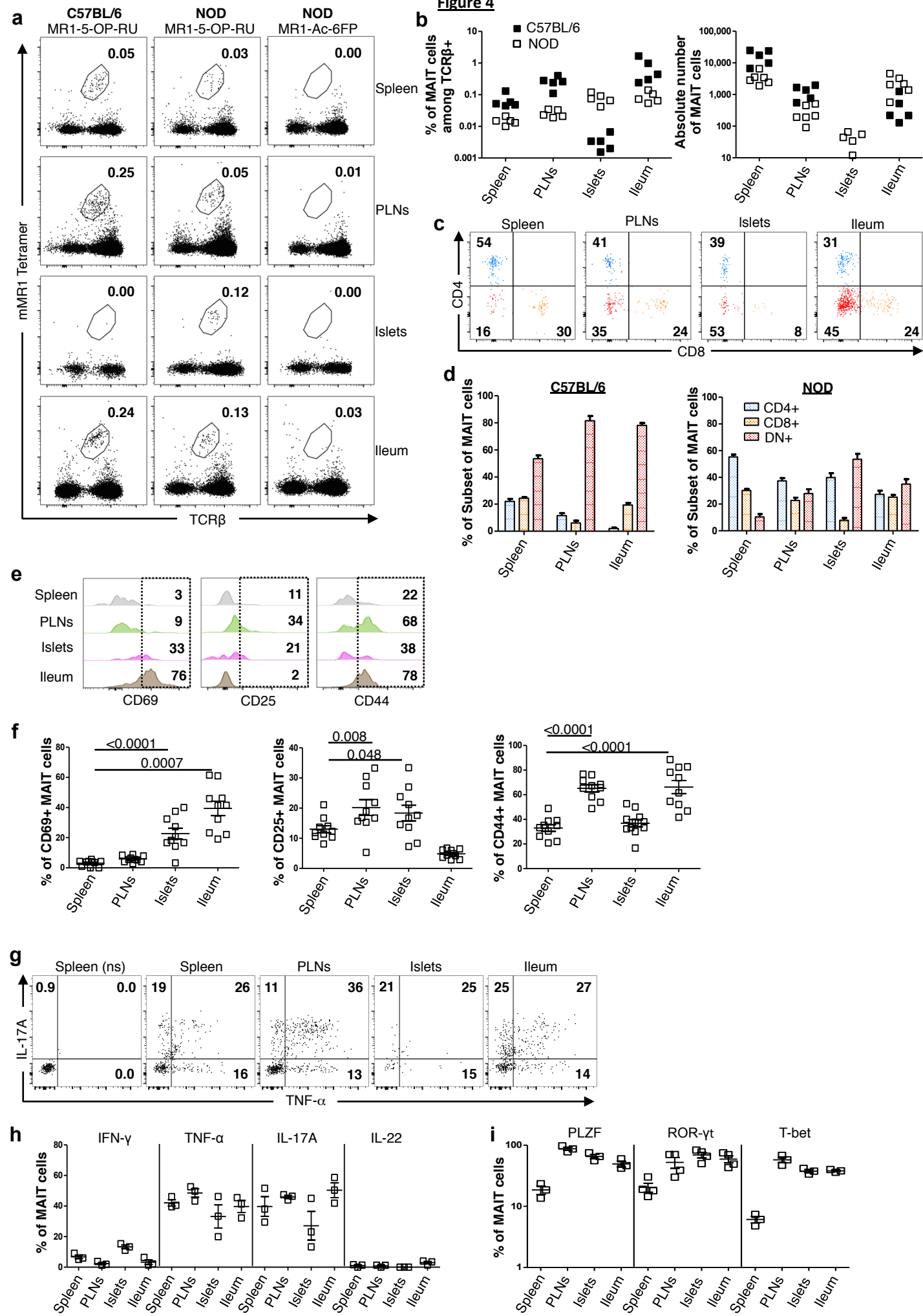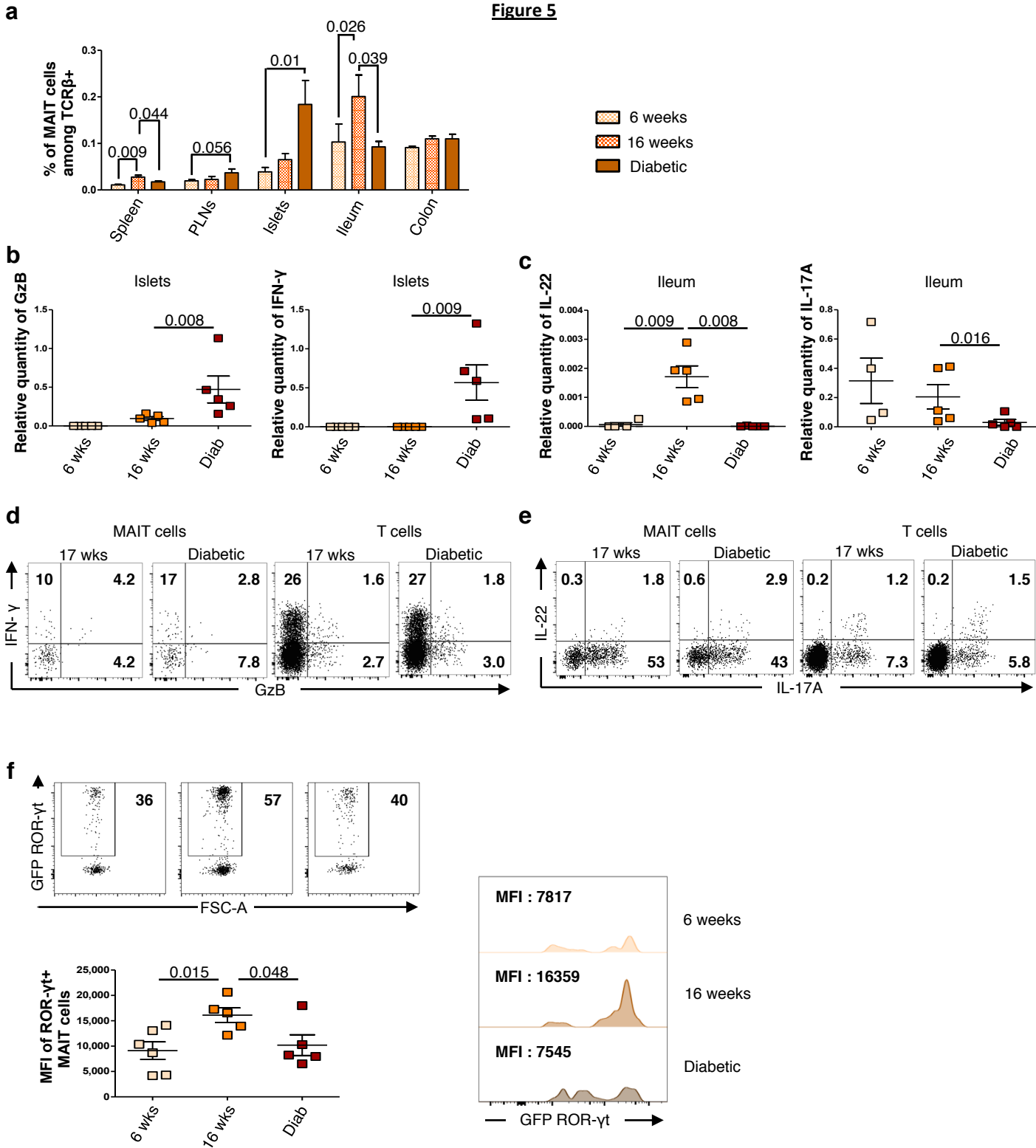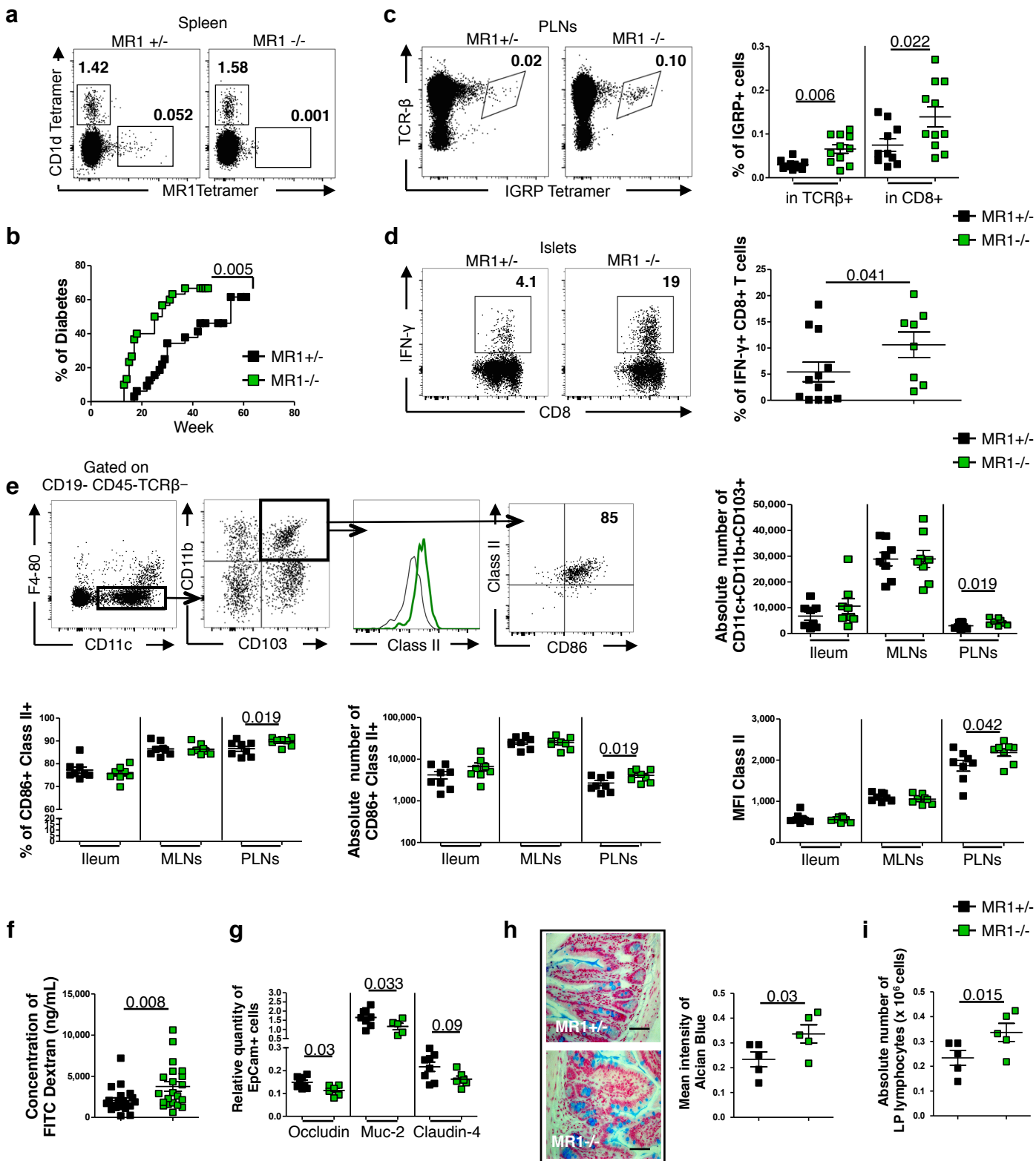
Figure 1

a

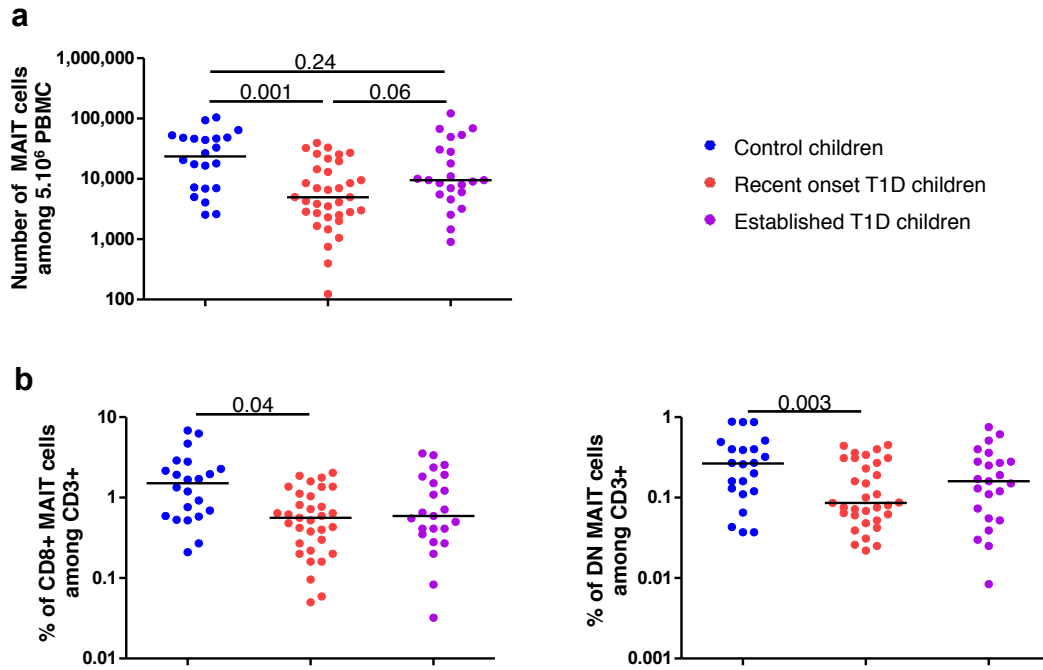% of MAIT cells among CD3+

- Control children
- Recent onset T1D children
- Established T1D children

0.0008
0.12
0.15

b

% of CCR6+ MAIT cells — 0.017

% of CD56+ MAIT cells — 0.004, 0.05

% of CD69+ MAIT cells — 0.12

% of CD25+ MAIT cells — 0.0003, 0.0003

% of PD1+ MAIT cells — 0.02

% of Bcl-2+ MAIT cells — 0.035

c

Control children

- 31.0% CCR6+CD56+
- 0.95% CD56+
- 3.42% NEG
- 55.40% CCR6+
- 0.40% CCR6+CD25+

- 1.14% CCR6+PD1+
- 0.41% CCR6+CD56+PD1+

- 2.91% CCR6+CD69+
- 3.77% CCR6+CD56+CD69+
- 0.68% Others (<0.36%)

Recent onset T1D children

- 17.75% CCR6+CD56+
- 0.48% CD56+
- 7.75% NEG
- 59.42% CCR6+
- 2.64% CCR6+CD25+
- 0.37% CCR6+CD25+PD1+
- 2.34% CCR6+PD1+
- 0.54% CCR6+CD56+PD1+
- 0.48% PD1+

- 4.01% CCR6+CD69+
- 2.56% CCR6+CD56+CD69+
- 1.66% Others (<0.36%)

Established T1D children

- 24.96% CCR6+CD56+
- 1.10% CD56+
- 5.60% NEG
- 57.2% CCR6+

- 2.36% CCR6+PD1+
- 0.90% CCR6+CD56+PD1+

- 0.41% CCR6+CD56+CD69+PD1+
- 3.33% CCR6+CD69+
- 2.79% CCR6+CD56+CD69+
- 1.35% Others (<0.36%)

Figure 2

Figure 3

Figure 4

Figure 5

Figure 6

a

b

Supplementary Figure 1 (a) Number of blood MAIT cells among five millions of PBCM from children with recent onset T1D (n=35), children with established T1D (n=23) as compared with control children (n=22). **(b)** Frequency of the subpopulation CD8+ and DN MAIT cells among T lymphocytes from children with recent onset T1D (n=41), children with established T1D (n=23) as compared with control children (n=22). P values were determined by Kruskal-Wallis test followed by the Wilcoxon rank sum test adjusted with the Holm method.
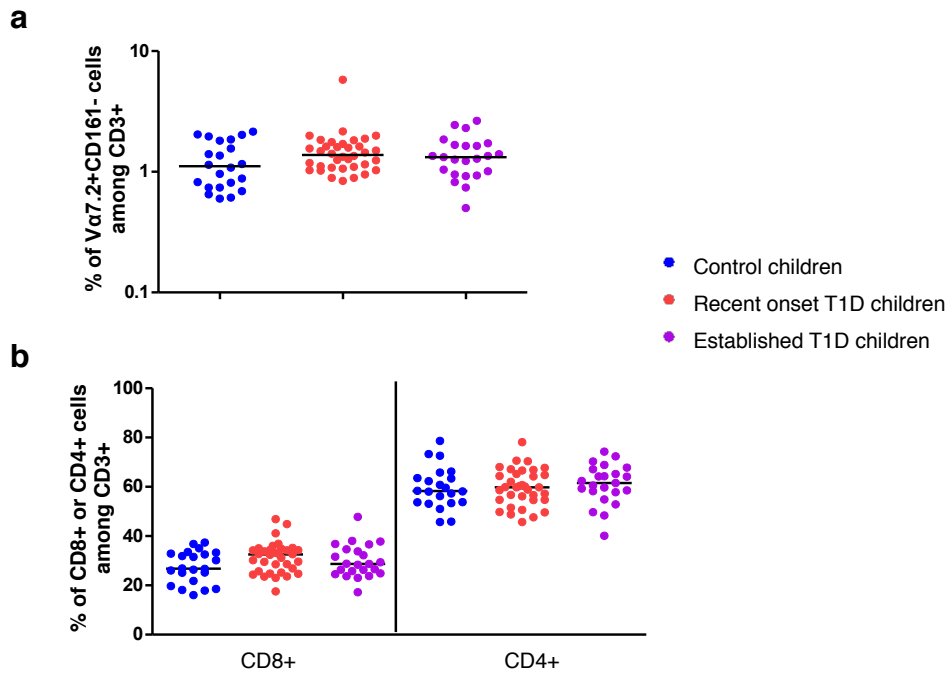
Supplementary Figure 2 (a) Frequency of Vα7.2+CD161- cells among T lymphocytes and **(b)** frequency of the CD4+ and CD8+ T lymphocytes from children with recent onset T1D (n=41), children with established T1D (n=23) as compared with control children (n=22). No significative differences as determined by Kruskal-Wallis test followed by the Wilcoxon rank sum test adjusted with the Holm method.
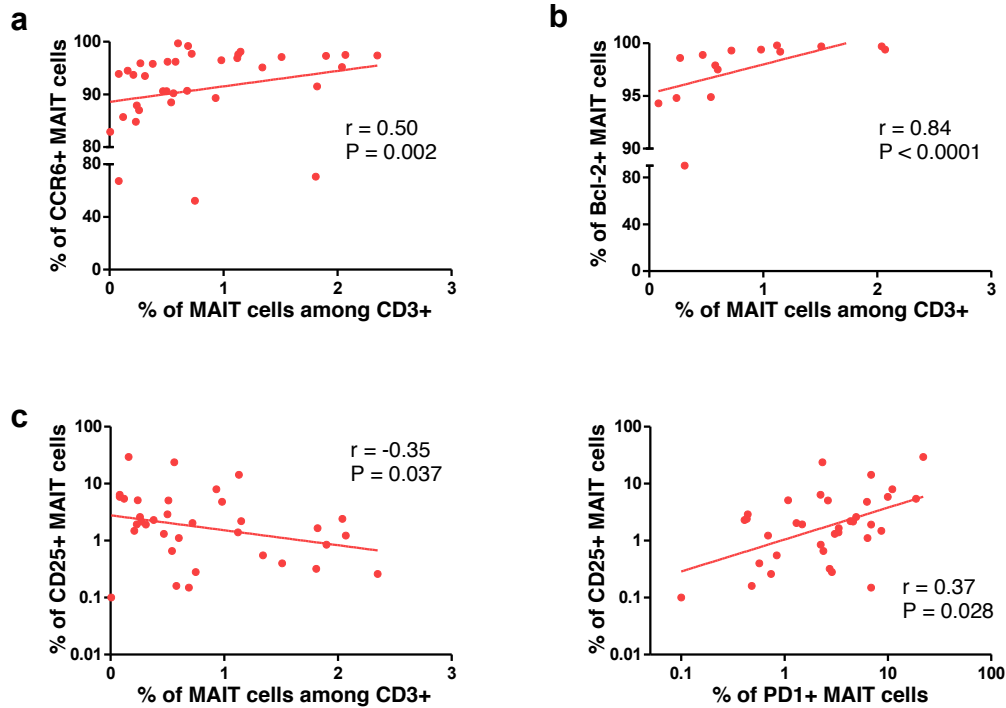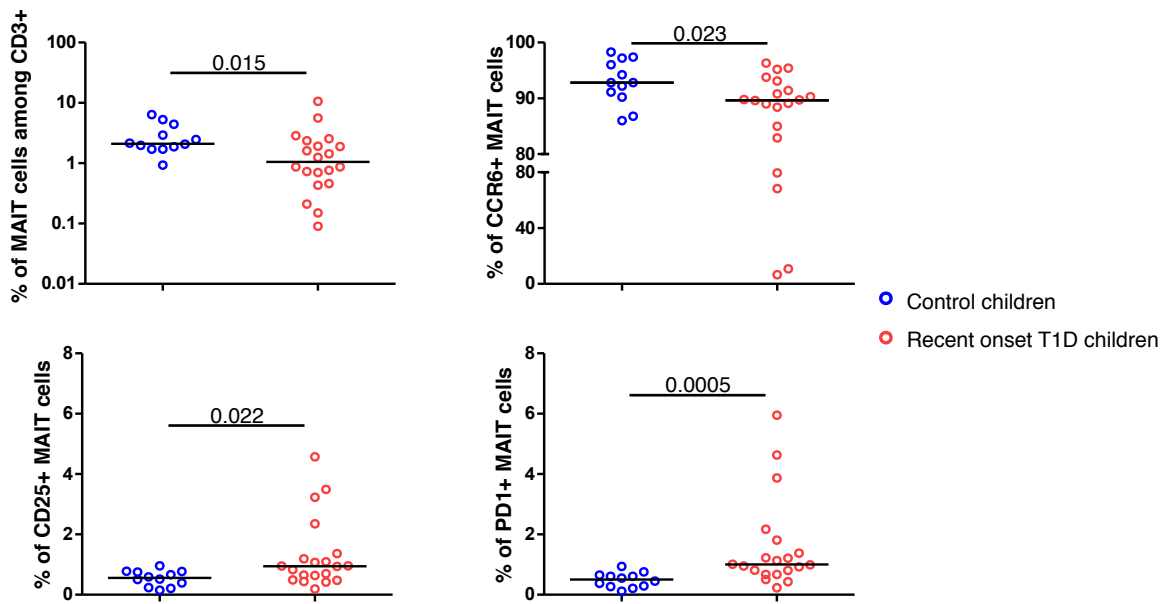
Supplementary Figure 3 (a) Correlation between frequency of MAIT cells expressing CCR6 and frequency of MAIT cells among T lymphocytes from children with recent onset T1D (n=41). **(b)** Correlation between frequency of MAIT cells expressing Bcl-2 and frequency of MAIT cells among T lymphocytes from children with recent onset T1D (n=15). Less samples were analyzed for Bcl-2 staining due to limited number of PBMC. **(c)** Correlation between frequency of MAIT cells expressing CD25 and frequency of MAIT cells among T lymphocytes from children with recent onset T1D (n=35). Correlation between frequency of MAIT cells expressing CD25 and frequency of MAIT cells expressing PD1 from children with recent onset T1D (n=35). P values were determined by Spearman test.
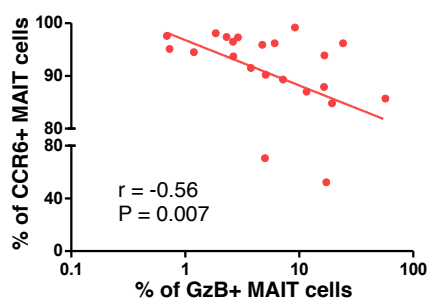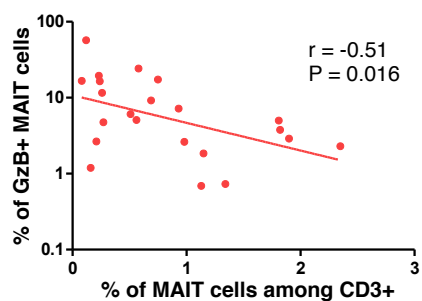
Supplementary Figure 4 Correlation between frequency of MAIT cells expressing GzB and frequency of MAIT cells among T lymphocytes from children with recent onset T1D (n=22). Correlation between frequency of MAIT cells expressing CCR6 and frequency of MAIT cells expressing GzB (n=22). P values were determined by Spearman test.
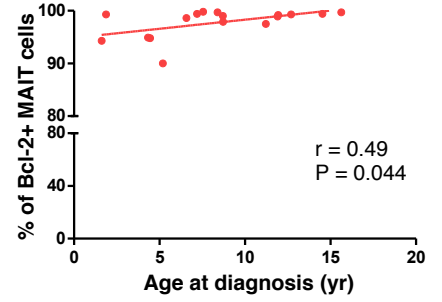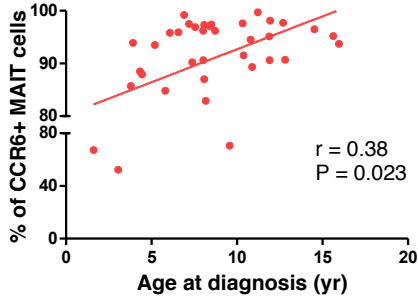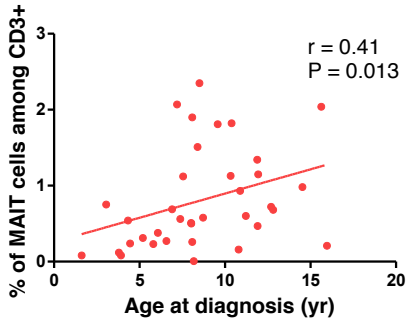
Supplementary Figure 5 Correlation between frequency of MAIT cells expressing different surface and intracellular molecules and the age of the children with recent onset T1D at the diagnosis. For surface staining n=41 and Bcl-2 analysis n=16. P values were determined by Spearman test.
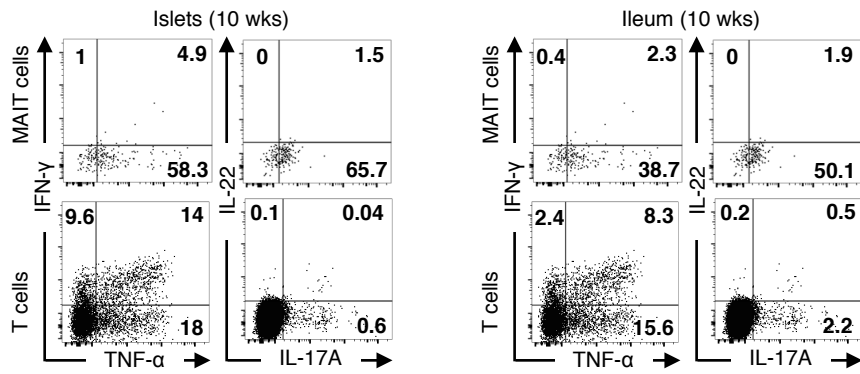
Supplementary Figure 5 Frequency of MAIT cells among T lymphocytes and frequency of MAIT cells expressing surface molecules after staining on frozen PBMC from children with recent onset T1D (n=20) and control children (n=12). P values were determined by Mann-Whitney Test.
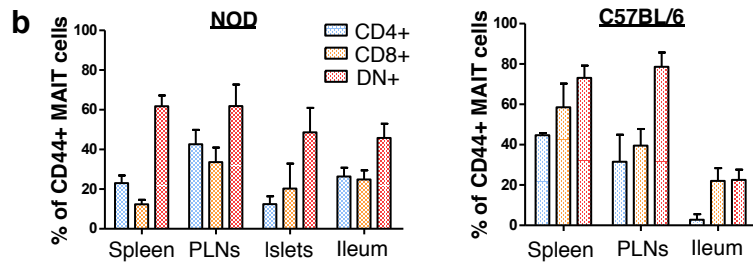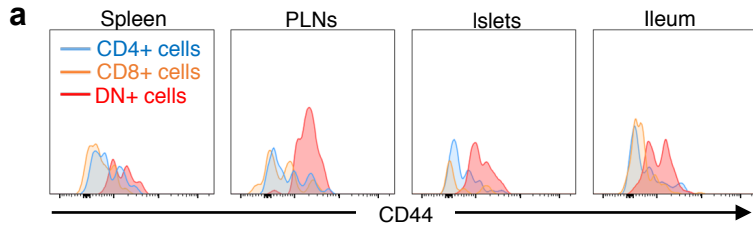
Supplementary Figure 6. CD44 expression on MAIT cell subsets in NOD and C57BL/6 mice. **(a)** Representative histogram of CD44 expression on CD4 (blue), CD8 (orange) and DN (red) subsets of MAIT cells from spleen, PLNs, islets and ileum from NOD mice. **(b)** Percentage of CD44+ MAIT cells in each subset of different tissues from 10 week-old NOD and C57BL/6 mice. Bars graphs depict mean ± SEM from at least 8 mice, analyzed in four (NOD mice) or two (C57BL/6) separate experiments.
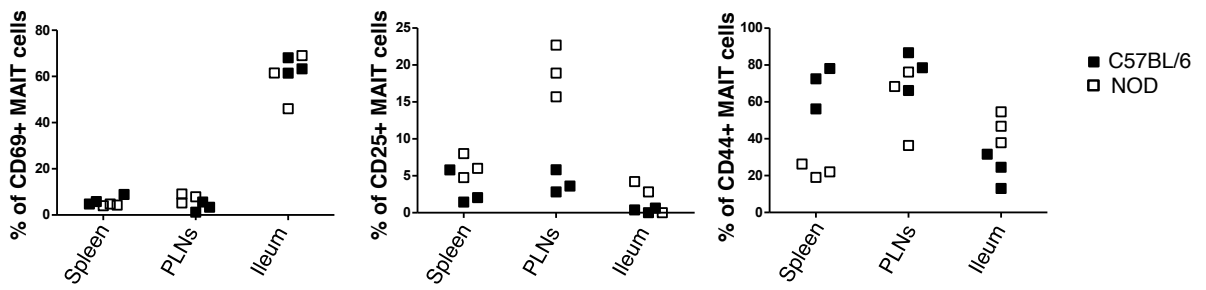
Supplementary Figure 7. Comparison of activation markers on MAIT cells between NOD and C56BL/6 mice. Frequency of CD69+, CD25+ and CD44+ MAIT cells from the spleen, PLNs and ileum from 10 week-old NOD (white) and C57BL/6 (black) mice. All data are representative of, at least, two separate experiments and each point represents a pull of two mice.

Supplementary Figure 8. Cytokine production by MAIT cells in NOD mice. Representative dot plots showing intracellular cytokine staining of MAIT cells from islets and ileum of 10 week-old NOD mice. MAIT cells are analyzed after PMA/ionomycin stimulation and labeled with MR1-5-OP-RU tetramer and then fixed and permeabilized before staining with IL-17, IL-22, TNF-α, IFN-γ mAbs. Conventional αβT cells are also analyzed as control. Data are representative of three experiments with combined total of 9 mice.
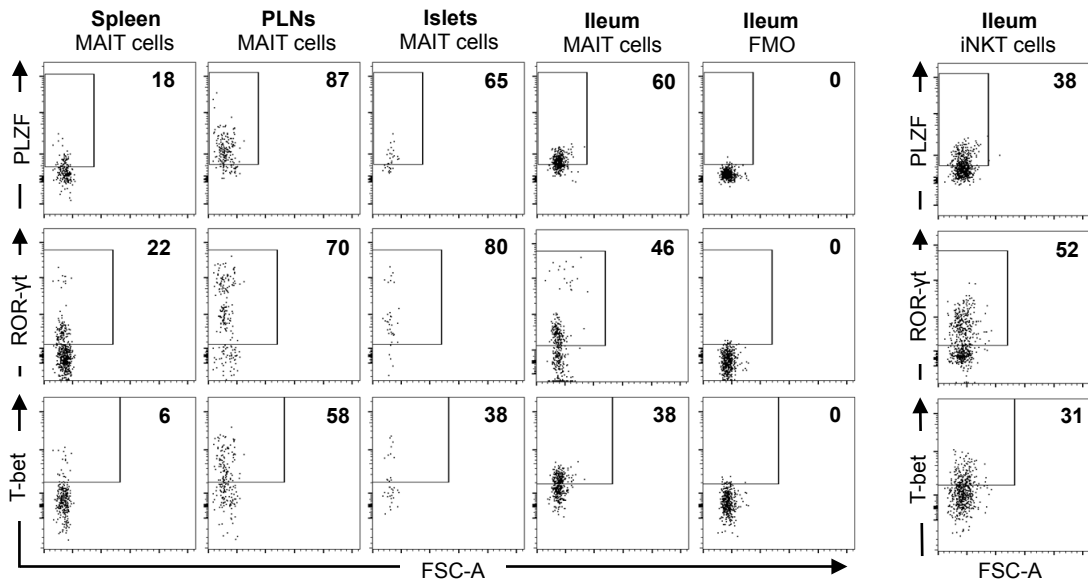
**Supplementary Figure 9**. MAIT cell expression of PLZF, ROR-γt and T-bet. Expression of the transcription factors PLZF, ROR-γt and T-bet by MAIT cells from the spleen, PLNs, pancreatic islets and ileum from 10 week-old NOD mice. Representative dot plots with indicated percentage of PLZF, ROR-γt and T-bet expression in MAIT and iNKT cells from different tissues. Dot plots for each marker show data concatenated from two or three individual mouse tissue samples from one experiment. Data are representative of two similar experiments. FMO, fluorescence minus one.
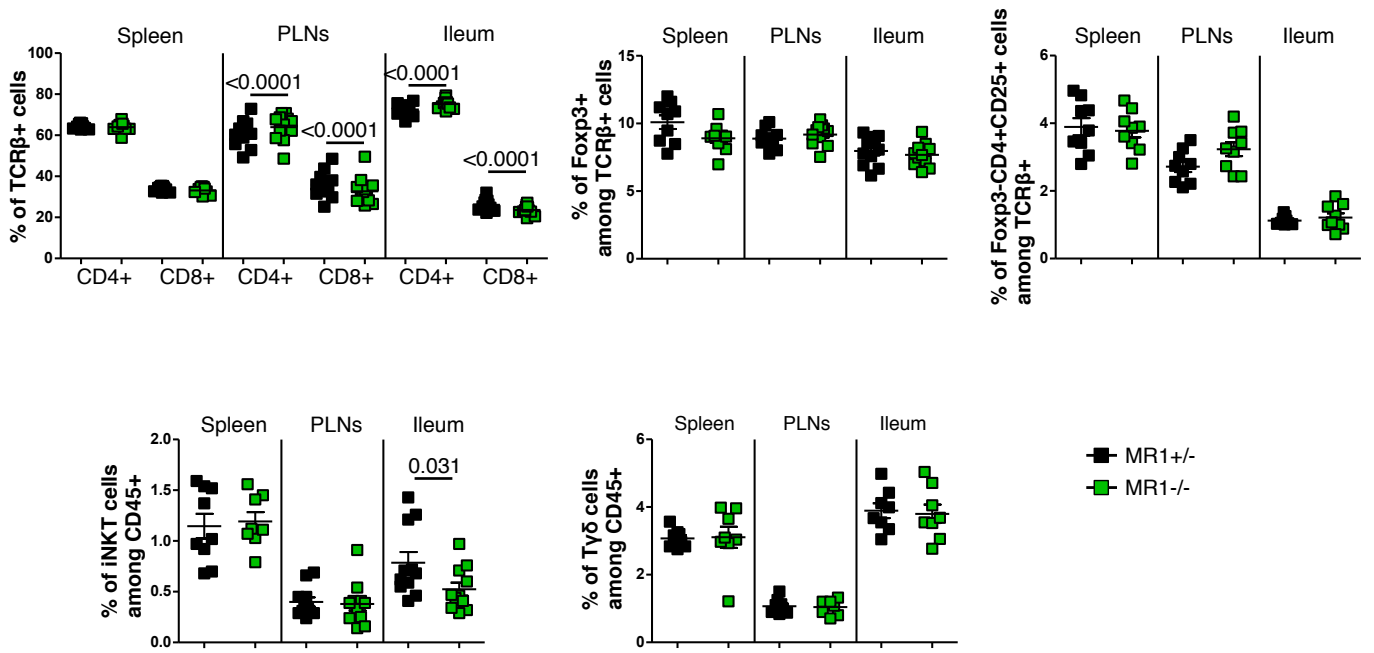
Supplementary Figure 10. Analysis of T cell populations in MR1-/- and MR1+/- NOD mice. Graphs showing the frequency of conventional CD4 and CD8 T cells, Foxp3 Treg cells, Foxp3- CD25+ CD4+ T cells, iNKT cells and γδT cells in PLNs and ileum as determined by flow cytometry. Analysis was performed on 8-12 mice per groups, in two independent experiments. P values were determined with Mann-Whitney test and bar represent mean ± s.e.m).
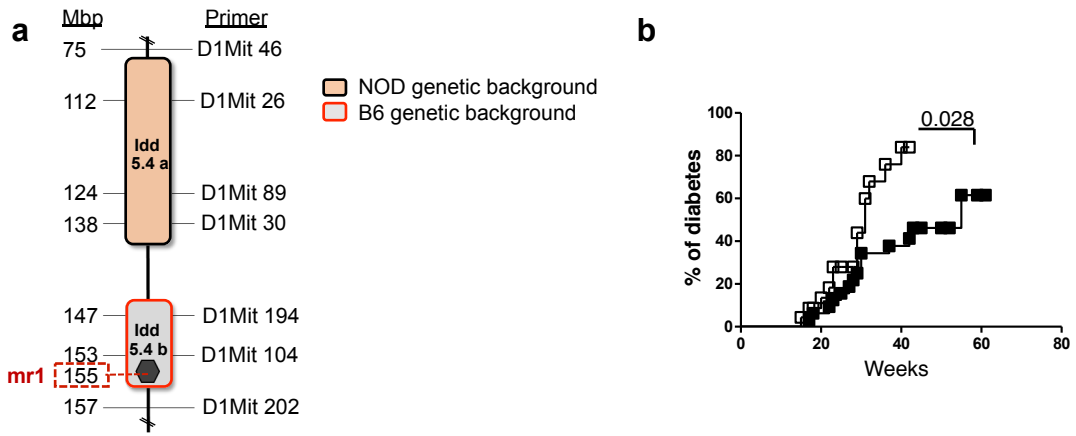
Supplementary Figure 11. Generation of MR1-/+ NOD mice. (**a**) Schematic diagram of mouse chromosome 1, mr1 gene and insulin dependent diabetes (Idd) 5.4a and b loci. (**b**) Cumulative incidence of diabetes of NOD (n=23) and MR1+/- NOD (n=32) mice. Statistical analysis was performed with Log rank-test.
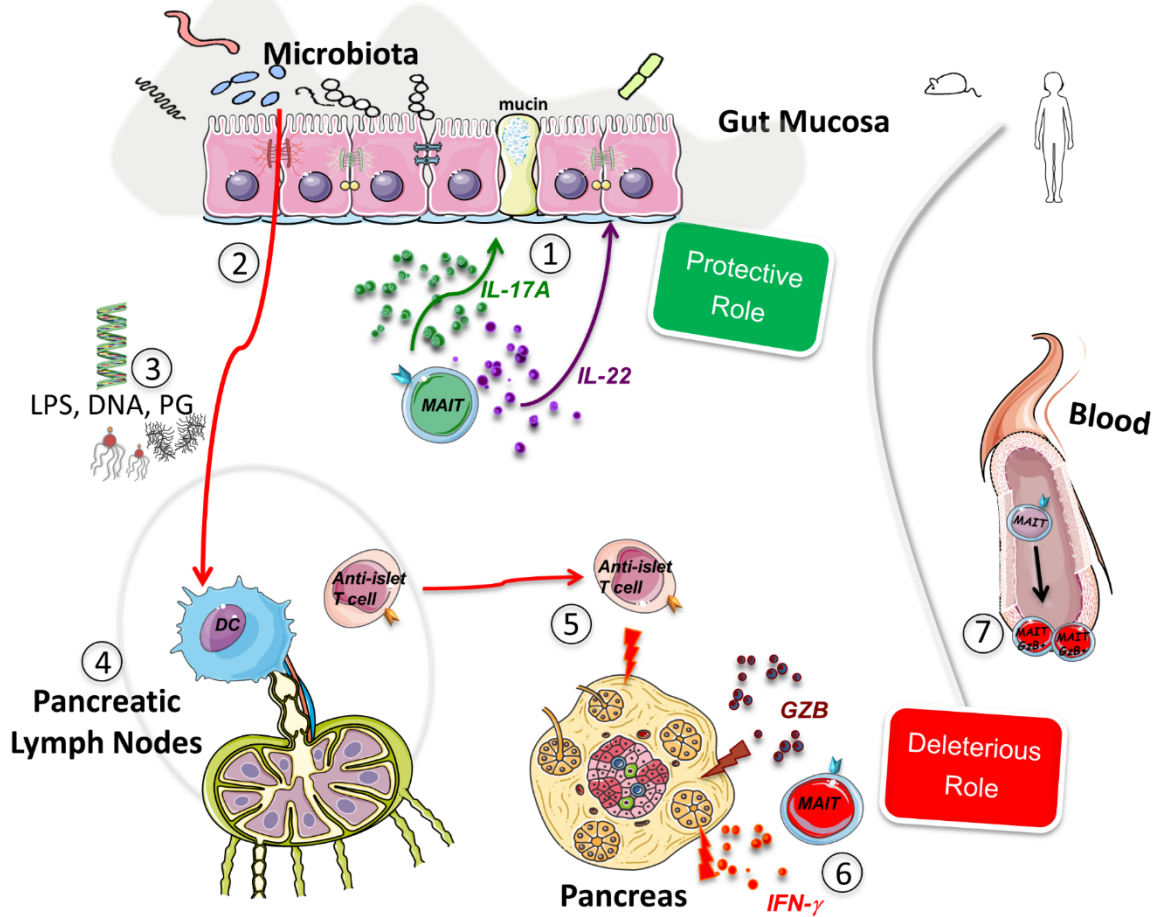
Supplementary Figure 12. Schematic view of the dual role of MAIT cells in the physiopathology of type 1 diabetes. MAIT cells recognize bacterial metabolites and changes of gut microbiota are associated with diabetes development. In the intestine of 10 week-old NOD females, MAIT cells produce IL-17A and IL-22, two key cytokines involved in the maintenance of gut mucosa integrity. (1) During disease progression, the production of both cytokines by ileal MAIT cell decreases, thereby dampening their protective role. (2) Moreover in MR1-/- NOD mice lacking MAIT cells several abnormalities are observed in the gut mucosa: increased gut permeability, decreased tight junction protein expression, alteration of mucus production and distribution, and increased lymphocyte infiltration in the lamina propria. (3) This defective intestinal barrier could favor the translocation of bacterial ligands such as lipopolysaccharide (LPS), DNA, peptidoglycan (PG) that could promote dendritic cell activation as evidenced by their increase MHC class II and CD86 upregulation in pancreatic lymph nodes. (4) Subsequently, these DC can activate autoreactive T cells recognizing beta-cell antigen. (5) These anti-islet T cells migrate to the pancreas where they produce IFN-g and thus destroy beta cells. This mechanism highlights the protective role of MAIT cells against T1D development. (6) However, MAIT cells can also participate to beta-cell death through their production of IFN-g and granzyme B (GzB). (7) Interestingly, in T1D patients there is an increase production of GzB by blood MAIT cells. While MAIT cells exert dual function, analysis of mouse models reveal the dominant protective role of MAIT cells in T1D.